

Advances in Materials and Technologies for Gas Sensing from Environmental and Food Monitoring to Breath Analysis

Angelo Milone,* Anna Grazia Monteduro, Silvia Rizzato, Angelo Leo, Corrado Di Natale, Sang Sub Kim, and Giuseppe Maruccio*

Gas sensing research experiences a worldwide revival in the last years. From one side, the emergence of novel sensing materials enables unprecedented capacities for improving the device performances. From the other, the increasing opportunities for applications impacting current societal priorities highly motivate further studies. Here, this field is reviewed with special attention to the emerging approaches and the most recent breakthroughs, challenges, and perspectives. In particular, this study focuses on: 1) the sensing layers analyzing recent trends toward nanostructured, low-dimensional and composite materials; and 2) the latest achievements and targets in terms of applications, from environmental monitoring to food aroma identification and quality control up to the healthcare sector with breath analysis and diseases diagnosis.

century^[1–5] with major focus on toxic and explosive gases in safety/security field and fire prevention, the amount of publications recently showed a strong increase from 2005 (Figure 1). This growing attention is associated to the broadening range of applications such as environmental pollution and air quality,^[6,7] food aroma identification, spoilage and quality control,^[8] and breath analysis and diseases diagnosis.^[9]

Crucial in this development was the availability of novel classes of materials (and technologies) to improve the sensors characteristics in terms of “3s”: sensitivity, selectivity, and stability. Indeed, in addition to inorganic and organic sensitive materials,

nanoscience and nanotechnologies provided a wide range of novel active, nanostructured, low-dimensional and nanocomposite materials. These state-of-the-art materials can open new frontiers in emerging fields such as healthcare through breath composition determination. In fact, this area demands sensors whose properties must fulfill very strict requirements, such as limits of detection up to ppb levels and the possibility to discriminate particular VOCs among more than 3000 gases that compose the humans exhaled.^[10] Here, we review progresses and perspectives of the field with special focus on active sensing materials, Volatile Organic Compounds (VOCs) and hazardous gases detection and most recent innovations enabling internet of food and volatilities.


1. Introduction

The field of gas sensing is experiencing a worldwide revival with the emergence of novel sensing materials and the increasing opportunities for applications impacting current societal priorities (Figure 1). After an early development stage in the past

A. Milone, A. G. Monteduro, S. Rizzato, A. Leo, G. Maruccio
Omics Research Group
Department of Mathematics and Physics “Ennio De Giorgi”
University of Salento, Institute of Nanotechnology CNR-Nanotec
INFN Sezione di Lecce
Via per Monteroni, Lecce 73100, Italy
E-mail: angelo.milone@unisalento.it; giuseppe.maruccio@unisalento.it

C. Di Natale
Department of Electronic Engineering
University of Rome Tor Vergata
via del Politecnico 1, Roma 00133, Italy

S. S. Kim
Department of Materials Science and Engineering
Inha University
Incheon 22212, Republic of Korea

 The ORCID identification number(s) for the author(s) of this article can be found under <https://doi.org/10.1002/adsu.202200083>.

© 2022 The Authors. Advanced Sustainable Systems published by Wiley-VCH GmbH. This is an open access article under the terms of the Creative Commons Attribution-NonCommercial License, which permits use, distribution and reproduction in any medium, provided the original work is properly cited and is not used for commercial purposes.

DOI: 10.1002/adsu.202200083

2. The Emergence of Novel Materials for Ultrahigh Sensitivity Applications

Two key elements for all chemical sensors are the transducer and the active layer which together allow us to transform analytes concentration in a measurable physical signal, then available to be processed and analyzed. In this respect, the range of transducing approaches includes optical sensors, chemiresistors and impedance sensors, transistor/diode (electronic) sensors, amperometric sensors, piezoelectric crystal sensors (e.g., based on quartz crystal microbalance [QCM] or surface acoustic wave [SAW] devices), calorimetric/thermometric sensors.^[11–14] However, in the last years, it is the field of active materials which remarkably underwent stronger innovation with the

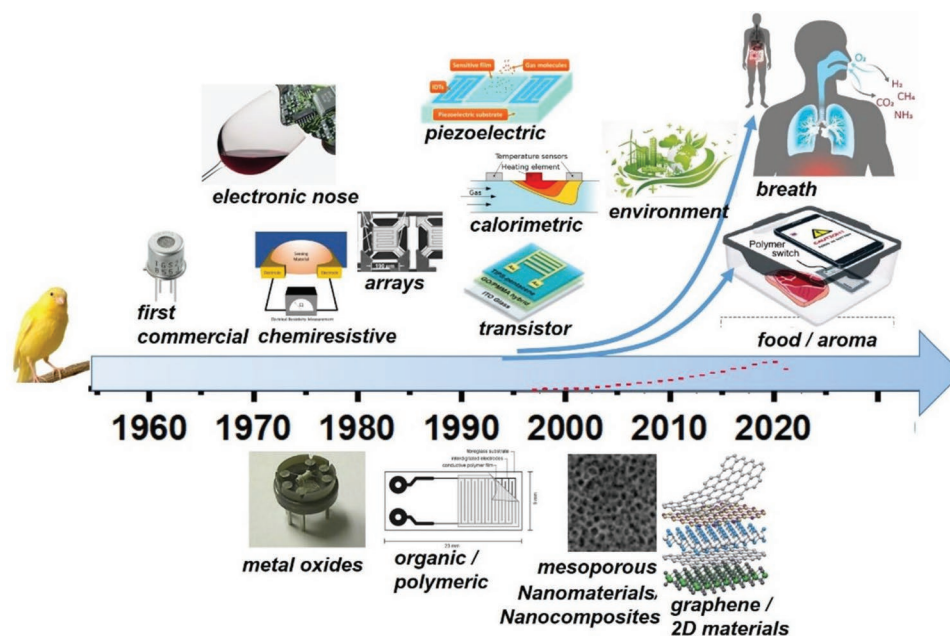


Figure 1. Trends in gas sensing and electronic nose research in terms of transducers, materials, and technologies from XIX century to date. The red dots within the arrows show the increase in gas sensing publications during the years.

emergence of novel materials (and combinations) for achieving ultrahigh sensitivity and enhanced specificity and stability leading miniaturized devices performances to approach those of benchtop methodologies such as mass spectrometry, ion mobility spectrometry, gas chromatography and infrared spectroscopy,^[15–17] so enabling unprecedented capacities for applications. For a further insight, it is useful to discuss progress in gas sensing materials in more detail.

2.1. Inorganic Materials

2.1.1. Metal Oxides Films

The first commercial gas sensor dates back to 1960s and employed metal oxides (MOx) as active layer.^[18–20] Then, various metal oxides films were investigated, such as SnO₂, TiO₂, WO₃, ZnO, Fe₂O₃ and In₂O₃ (Figure 2a). In this class of materials, the sensing mechanism depends on oxygen vacancies and a modulation of the available charge carriers and depletion regions at the active surface.^[14] However, in most of the cases, a similar surface modification is induced by different analytes, resulting in poor selectivity.

Metal oxide sensors generally need a pre-heating phase in which oxygen adsorbs and ionizes on the surface leading to O ions which are reactive with activated hydrogen, dehydrogenate hydrides, and hydrocarbons.^[6,7,16,21] As a result, the material becomes sensitive to the gas analyte but the process requires high working temperatures (100–400 °C), which are responsible for high power consumption, baseline drift, and oxidation of analytes.^[14] Sensitivity and specificity are also influenced by the operating temperature.^[16]

In general, the resistance variation depends on the sensing material (n-type or p-type metal oxide) and the gas analyte

(oxidizing or reducing).^[6,22,23] Both n-type and p-type oxide semiconductors can adsorb oxygen, but exhibit different conduction trends in their response. From a general point of view, the most commonly used oxides are n-type materials, such as ZnO^[23] (Figure 2a). In this case, if the sensor is exposed to air, oxygen molecules adsorb on the surface and collect electrons from ZnO conduction band, resulting in chemisorbed reactive oxygen species (O₂⁻, O²⁻, O⁻) able to react with reducing gases, such as acetone.^[21] So, when the acetone vapor is introduced, a chemical reaction occurs, releasing electrons back into the conducting band and then causing a measurable resistance decrease. On the other hand, oxidizing gases react directly with the bulk material (instead than the formed O ions) but still modifying the conductivity.^[22]

Because of analyte-induced changes in their electrical properties, metal oxides are very suitable for resistive or impedance-based read-out and an important milestone was the development of the first chemiresistive gas sensors at the beginning of the 1970s. In Figure 2b, the layout of a typical chemiresistor is shown, consisting of two (often interdigitated) electrodes, connected by the active layer. Regarding impedance sensors, the structure can be similar, but the typical response curve takes the form of a Nyquist plot (Figure 2c), containing information on both resistance and capacitance changes, which can be extrapolated by fitting with an equivalent circuit.

Easiness in miniaturization and stability (thanks also to regeneration during the heating phase) are among the major advantages of this kind of devices. E-noses are today available using this technology, especially for air quality control. Another interesting application for metal oxide gas sensors is food aroma identification: considering that the human nose is less responsive to higher oxidized volatiles,^[16] artificial sensors could be helpful in this field (see also Section 3.3).

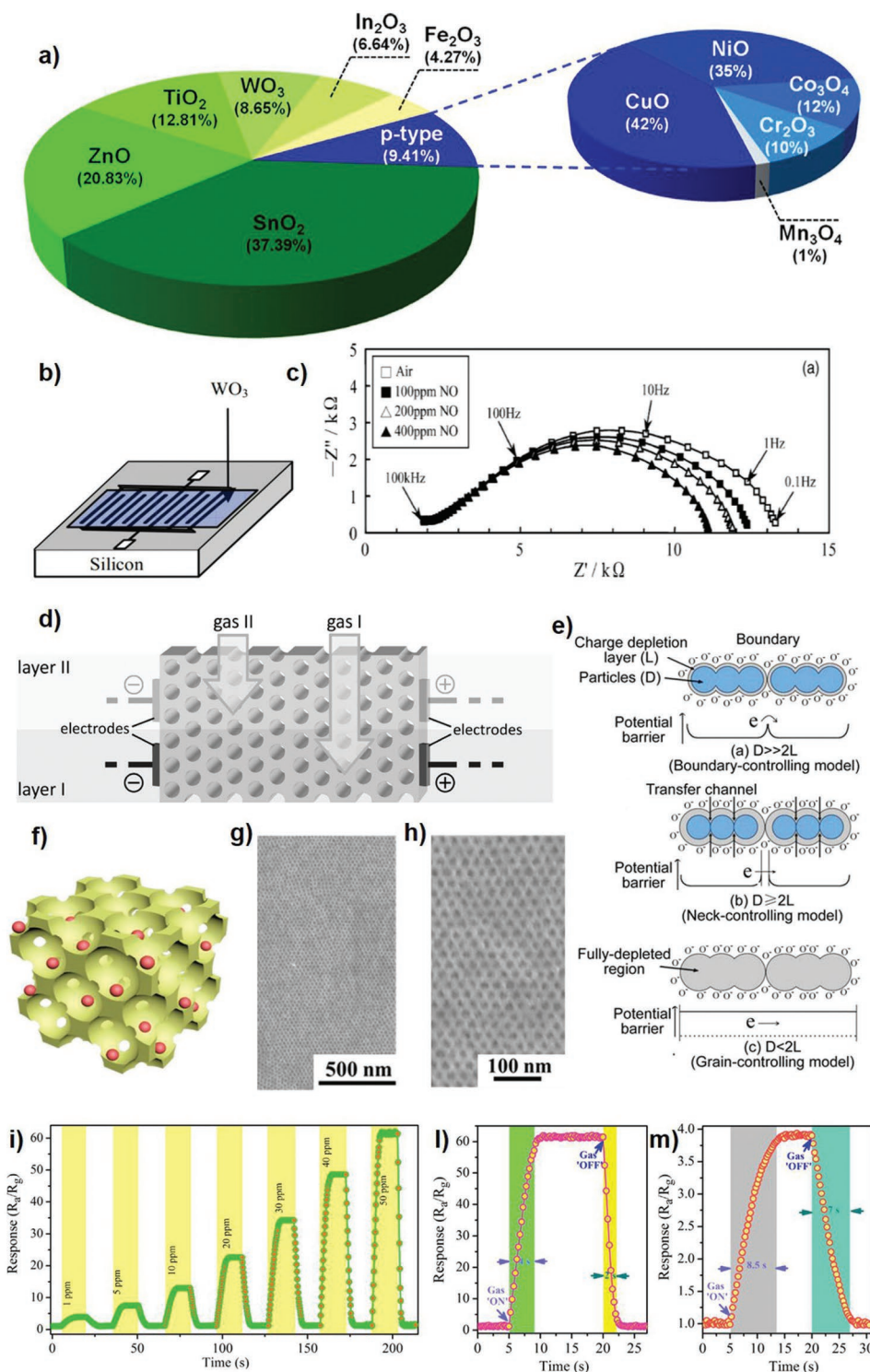


Figure 2. a) Pie chart illustrating the use of n-type and p-type metal oxides materials in gas sensing research (reproduced with permission.^[23] Copyright 2014, Elsevier B.V.); b) schematics of a typical chemiresistors (e.g., based on WO_3 -films) (reproduced with permission.^[55] Copyright 2007, IEEE); c) response of a solid-state impedance NO_x gas sensor upon NO exposure (reproduced with permission.^[56] Copyright 2003, Elsevier B.V.); d) Illustration of gas sensing through a mesoporous material with different analyte percolation ability (reproduced with permission.^[24] Copyright 2013, Royal Society of Chemistry); e) grain size effect in n-type semiconducting metal oxide gas sensors (reproduced with permission.^[57] Copyright 2012, MDPI); f–h) crystal-line ordered mesoporous WO_3/Pt composites schematic and FEGEM images (reproduced with permission.^[47] Copyright 2018, Elsevier B.V.); i) typical response curves of In(III)- SnO_2 loaded cubic mesoporous graphitic carbon nitride sensor when exposed to toluene vapors at a working temperature of 200 °C; l, m) response to 50 ppm and 1 ppm toluene gas at 200 °C (reproduced with permission.^[53] Copyright 2018, Elsevier B.V.).

2.1.2. Mesoporous Metal Oxides (and Zeolitic Imidazolate Frameworks)

Mesoporous materials present nanoscale pores and large surface-to-volume ratios which are useful to increase sensitivity (Figure 2d).^[24] Porous semiconducting metal oxides were employed in gas sensing since they combine high gas accessibility with availability of larger sensing areas.^[25–34] To provide a measurable response, the target gas must penetrate as much as possible into the porous layer in order to induce a larger signal change (Figure 2d). However, supposing that an analyte penetrates more than another, this process can be also exploited to improve selectivity in their discrimination since gas diffusivity strongly depends on pore size (Figure 2d) with the diffusion coefficient D_k proportional to the pore radius r :^[24]

$$D_k = \frac{4}{3}r \sqrt{\frac{2RT}{\pi M}} \quad (1)$$

where R is the universal gas constant, M the molecular weight, and T the absolute temperature. Indeed, mesoporous materials can also be adopted as filter layers integrated on sensors (Figure 2d). In this way, the presence of catalytically active species and the gas diffusion through porous layers can be exploited to separate certain gas molecules from others (i.e., suppression of H_2O or O_2 permeation), enhancing the sensor's selectivity.

The grain/pore size effect is another relevant aspect in determining the response^[22,35] (Figure 2e), due to the role of charge depletion layers and inner regions in defining the relevant potential barriers and transport model. By heating a mesoporous metal oxide, as a consequence of the O ions adsorption, a depletion layer forms. The depletion layer is responsive to the gas concentrations in the environment, instead, the interior parts do not contribute to the sensing; thus, best results are obtained when sizes are in the few nanometers range.^[7,23,24] In this case, the most conductive part is the internal/core region, and it is necessary to limit it in comparison to the depletion layer to maximize the sensor's sensitivity. An approach to improve the sensitivity of porous materials films consists in using hierarchical and hollow oxide structures where the microscale pattern composed of smaller building blocks provides an effective gas diffusion path via nanoporous architectures with a high surface area.^[36]

Mesoporous material-based sensors can exploit different sensing principles, using resistance, capacitance, optical or gravimetric signals. SiO_2 , WO_3 , and In_2O_3 mesoporous materials are among the most employed to implement chemiresistors for the detection of organic volatiles.^[24,37–44] A bimodal pore size distribution was engineered by Li et al. in mesoporous WO_3 reaching ultrahigh sensitivity (20 ppb) and this approach can lead to new strategies to tune absorption, separation, diffusion, and catalytic properties of the mesoporous films.^[45] Recently, a study on pore size influence on the performance of acetic acid sensors was reported.^[46] A recent research trend in the use of mesoporous materials for gas sensing concerns the use of hybrid materials, for example, combining Pt nanoparticles with WO_3 semiconductors^[47] (Figure 2e–g). Quang and co-workers employed mesoporous p-type Co_3O_4 active layers to

detect H_2S .^[48] In other studies, ferrite materials were used as sensing layers.^[49,50] Other promising compounds are zeolitic imidazolate frameworks structures (ZIFs), which are a sub-family of metal-organic frameworks (MOFs) characterized by ultrahigh porosity, structural and chemical tunability and great equivalent internal surface areas.^[51] Mesoporous silica materials have been also used as host matrices to create optical gas sensors.^[24]

The research trend on MO_x -based sensors is today mainly focused on addressing their limitations in terms of high working temperatures, poor selectivity, and stability toward humidity. Today, mesoporous structures permit to reach sub-ppm limit of detection (LOD) levels and open the way toward frontier applications requiring this level of sensitivity (Figure 2e,f). The high working temperatures are among the main disadvantages often associated with metal oxides-based mesoporous materials, making these sensors not ideal for explosive gases detection. Moreover, on the long time period, the high temperatures can also lead to the collapse of mesoporous structures and/or to the film cracking.^[52] In this respect, it is relevant to mention the toluene sensor based on $In(III)-SnO_2$ loaded cubic mesoporous graphitic carbon nitride recently reported to exhibit high sensitivity and fast response (Figure 2i–m) at low temperature.^[53] Low temperature operation is useful to allow field use for a large set of analysis.^[54] In this respect, reducing the size to the nanoscale is a suitable strategy which permits us to exploit the concept of self-heating. Due to its relevance in current research, gas sensors based on nanomaterials and nanoheterostructures merit a separate discussion (see Sections 2.1.3 and 2.1.4, respectively).

2.1.3. Metal Oxides Nanomaterials

The use of nanomaterials in gas sensors is more recent but very attractive because of their large surface-to-volume ratio which results in an increased number of active sites and can provide ultra-high sensitivity, short (ms) response times, and good reversibility and selectivity.^[19,58–75] Then, in the case of metal oxides materials, nanostructures can also enable room temperature operation in contrast to their bulk form which typically requires heating elements. As an example, the use of SnO_2 nanotubes allowed NO_x detection below 10 ppb^[76] under room temperature operation. This improved performance with respect to thin films is attributed to higher surface-to-volume ratios and an easier access to sensing active sites. Notably, in the case of nanomaterials, self-heating operation was also demonstrated as an effective strategy to operate the sensors without an external heat source.^[77–80] The resulting reduction in energy consumption makes these devices advantageous for low cost, indoor, and safety applications (i.e., explosives detection, and H_2).^[67]

SnO_2 nanowires were largely investigated in the last years for gas sensing purposes. In this context, S.S. Kim group examined the influence of In- and Sb-implantation, femtosecond laser irradiation and coating with porous alumina nanomembrane on gas sensing, operating temperatures, recovery times and humidity resistance^[81–84] (Figure 3a,b). In particular, implantation was reported as a potential strategy for improving

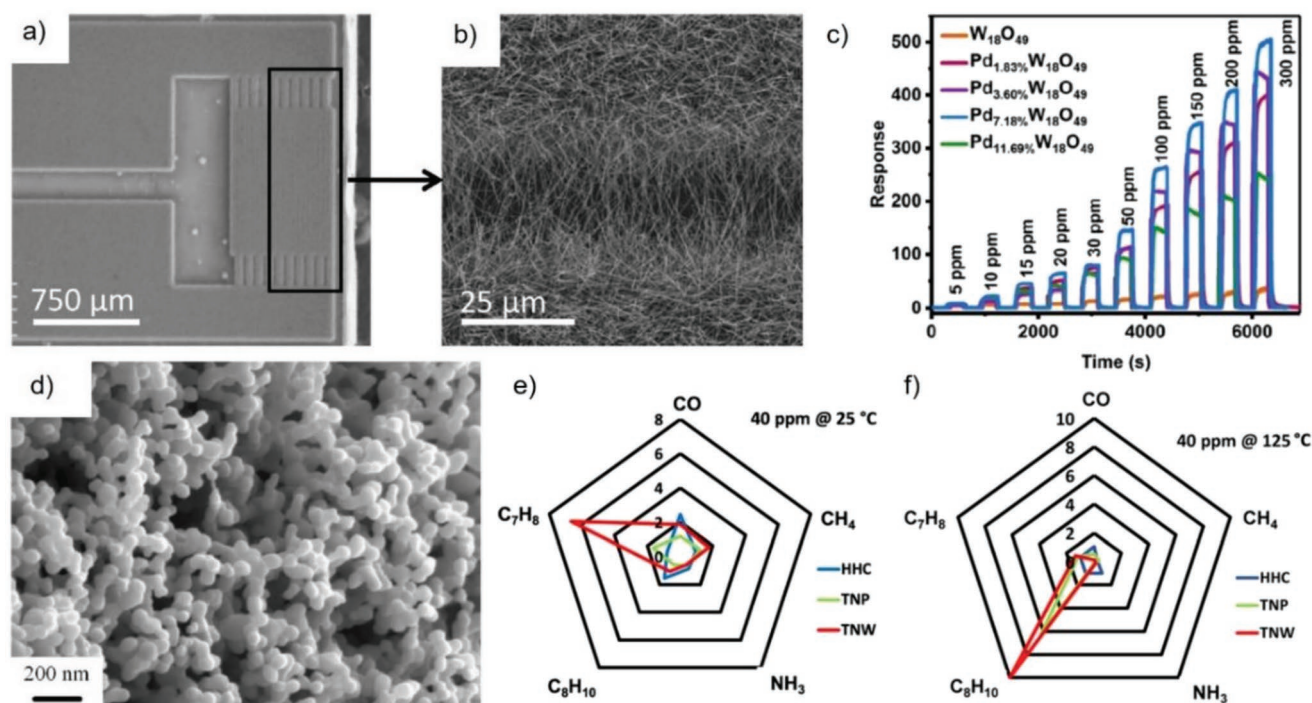


Figure 3. a,b) SEM images of humidity-resistant gas sensors based on SnO₂ nanowires: top view and synthesized nanowires (reproduced with permission.^[83] Copyright 2021, Elsevier B.V.). c) Pd_xW₁₈O₄₉ nanowires responses to different concentrations of acetone at 175 °C. (reproduced with permission.^[87] Copyright 2021, American Chemical Society); d) SEM images of a ZnO nanoparticle network fabricated using a porous metal organic framework as precursor (reproduced with permission.^[98] Copyright 2021, Elsevier B.V.). e,f) Selectivity plot of different TiO₂ nanostructures-based sensors to 40 ppm gas concentration at 25 and 150 °C, respectively (reproduced with permission.^[93] Copyright 2021, American Chemical Society).

the performance inducing the formation of structural/surface defects and a core-shell structure beyond affecting also carrier concentration. Laser irradiation was instead shown to induce radial modulation, increase the surface area and lead to formation of homojunctions and oxygen vacancies in the SnO₂ NWs. SnO₂ nanowires were integrated by Lu et al. in devices for sensitive H₂ detection with linear response from 2 ppm to 100 ppm and the authors achieved a reduction of the operating temperature (from 250 to 150 °C) and improved response and recovery time by doping them with palladium.^[85] WO₃ nanotubes and nanowires were also used^[86] and Pd doping was employed by Li et al. to induce oxygen vacancies and enhance the acetone sensitivity in WO₃ nanowires^[87] (Figure 3c). In ref. [88], SnO₂ nanowires were shown to enable the recognition of the fingerprints of seven different gas analytes by measuring the dynamic resistance of a single sensor at five different temperatures. Specifically, a support vector machine (SVM) was used to analyze the entire dataset leading to classification with sensitivity and precision of 94.3% with an average error of 18.4% in the concentration levels.

Different works reported also light illuminated devices in the ultraviolet-visible (UV-vis) range^[89,90] and in ref. [91] visible-light-modulation resulted in dual gas selectivity between NO₂ and NH₃ at room temperature. Furthermore, pulsed UV-radiation was shown to lead to performance enhancement in SnO₂ nanowires sensors by Hung et al.^[92]

Stability in humid conditions is highly sought being humidity a major challenge for gas sensor reliability and stability. Furthermore, humidity is significantly present in

ambient condition and breath analysis applications. In this respect, large surface-to-volume ratios combined with high temperatures can determine limitations in the use of sensors based on metal oxide nanomaterials, but a possible solution comes for their ability to operate at low temperature or to be stabilized in order to provide humidity resistant devices. For example, a porous alumina nanomembrane coating was shown to enhance humidity resistance and improve gas response, stability, and recovery times in humid conditions (RH from 30% to 90%) in the case of sensors employing SnO₂ nanowires conformally coated by means of a molecular layer deposition technique.^[83] Furthermore, Tshabalala and co-workers reported humidity-stable toluene (C₇H₈) and xylene (C₈H₁₀) gas sensors based on TiO₂ nanostructures, investigating nanoparticles (TNP), nanowires (TNW) and sea-urchin-like hierarchically arranged nanostructures (HHC) with the last two classes exhibiting high surface area and interconnected pore distribution^[93] (Figure 3e,f). Jeon and co-workers instead investigated gas sensors based on ZnO nanowires^[94] and employed atomic layer deposition to achieve a conformal coating with ZnO nanofilms and control the surface area (critical up to 50 ALD cycles) and the oxygen vacancies density (critical for >50 cycles) in order to enhance the gas response to NO₂, NH₃, CH₄, H₂, and C₃H₈. Si nanowires and Te nanotubes permitted to detect a concentration below 1 ppm of NO and NO₂, respectively.^[95,96] Black phosphorus nanowires were investigated by Jiang et al.^[97] ZnO nanoparticle networks were employed by Xia et al. for ethanol detection analyzing the influence of annealing and operation at different temperatures.^[98]

In general, it is not easy to provide design rules and preferences; however, it is typically preferable to increase the active layer surface-to-volume ratio and consider eventual gas catalysts and/or materials affinities according to the target analyte.

2.1.4. Nanoheterostructures Based on Metal Oxides and Noble Metals

In order to combine the properties and advantages of different nanomaterials, nanoheterostructures attracted large interest.^[99–105] For example, SnO₂/ZnO and ZnO/SnO₂ heterojunctions and SnO₂/SnO₂ and ZnO/ZnO homojunctions were investigated by Duoc et al. for room temperature NO₂ sensing at ppt level (Figure 4a)^[106] while Kim et al. studied the influence of shell thickness in ZnO-SnO₂ core-shell nanowires on CO, C₆H₆, and C₇H₈ gas sensitivity reporting best sensitivity and fastest response for a 40 nm shell thickness with dominant sensing mechanism related to radial modulation and shell/NW volume ratio^[107] (Figure 4b–d). Core-shell nanowires were also explored in other works.^[108]

Within the studies on nano-heterostructures, nanoparticle-decorated nanowires play a key role, often in the form of noble metal nanoparticles and metal oxide nanowires. In this respect, Cai and co-workers investigated the best amount of Pd nanoparticles on SnO₂ nanowires for optimizing sensitivity and selectivity to hydrogen thanks to the Pd catalytic effect and Schottky junctions formation at the heterointerfaces.^[109] Similar studies were performed by Kim group using SnO₂ and ZnO NWs and Pt and Pd nanoparticles (NPs).^[80,110–113] In general, the generation of heterointerfaces, electronic/chemical sensitization by noble metals and adsorption phenomena contribute to improve sensitivity and selectivity (Figure 4e–i). Decoration with noble metal nanoparticles was also employed on amorphous In–Ga–Zn–O thin-films and β-Ga₂O₃ nanowires for NH₃ and CO gas sensors, respectively.^[114,115] Colloidal lithography is another method to produce metal nanoparticles arrays on nanoporous thin films for gas sensing.^[116,117] In a somehow complimentary approach, SnO₂:NiO thin films were sputtered on Au NPs arrays for fabricating NO₂ sensors.^[118] For hydrogen sensing, Pt-functionalized PdO nanowires were also investigated.^[119] In other studies, CeO₂, AgO₂, and CoOx nanoparticles were employed to decorate SnO₂ and WO₃ nanowires^[120–122] or Co₃O₄ nanoparticles were incorporated into In₂O₃ 1D ribbons.^[123] A systematic study on formaldehyde sensing with WO₃ nanowires decorated with various metal nanoparticles was performed by Bouchikhi et al. and the radar plot reported in Figure 4e demonstrates as compositional modifications (and UV irradiation) allow us to tune the device response.^[124] Nano-heterostructures also led to a boost in gas sensors properties with impact on advanced applications. As an example, in ref. [125], In₂O₃/Au nanorods (NRs) devices reached sensitivity to ethanol concentrations ranging from 0.05 ppm to 650 ppm (Figure 4l–n) and these features were used to detect VOCs in exhaled breath (see Section 3.4 for further details).

Beyond chemiresistors, other transducing approaches were employed for implementing nanomaterial-based gas sensors, such as impedance sensors, field-effect

transistors, optical sensors, and piezoelectric sensors. Within the last class, SAW sensors employing palladium and copper nanowires have been reported for fast response hydrogen detection with a LOD of 7 ppm.^[126] In this case, nanowires trap the hydrogen molecules by adsorbing them and result in a frequency shift in SAW resonance mode.

2.2. Organic Compounds and Polymers

2.2.1. Conductive Organic Compounds and Polymers

The use of organic compounds and conducting polymers in gas sensing started in the early 1980s.^[127] In general, they are useful for realizing room-temperature gas sensors with good sensitivities and short response times (generally tens of seconds). The large versatility of organic chemistry allows for the preparation of countless molecules and polymers of different affinity and selectivity with volatile compounds. These materials are generally based on sorption mechanisms and they can be synthesized in order to modulate a number of different interactions such as van der Waals forces, hydrogen bonds, CH-π, π-π interactions, and coordination bonds.

Conductive organic materials are based on conjugated molecules presenting π and π* bonds with delocalized electrons enabling charge transport along the polymer backbone chain, mainly via hopping mechanism. To increase their conductivity, carrier density can be modified via doping. Gas sensitivity comes from changes in electrical conductivity due to doping–dedoping processes, variations in optical absorption, and polymer weight modifications. By adjusting the chemical properties, it is possible to change the affinity to different gases. Moreover, a further advantage is that chemical reactions occurring with gas analytes are generally reversible. These materials present good mechanical properties and can be made soluble, allowing the use of inexpensive techniques (such as drop casting, spin coating, or blade deposition) for a facile fabrication of sensors, even on flexible substrates. On the other hand, drawbacks comprise the possible influence of many ambient factors to their response, long-time instability (e.g., due to dedoping of conducting polymers because of environment interaction, i.e., moisture), and low selectivity. In particular, the humidity in a real environment strongly affects the electrical properties and responses,^[14] although competitive adsorption occurs between water and the analyte was also observed to increase sensitivity in some reports.^[12]

The list of conductive polymers most used in chemiresistors for gas sensing includes polyacetylene (PA), polyaniline (PAni), polypyrrole (PPy), polythiophene (PTh), and their derivatives (Figure 5a). From 1987 to now, PAni (polyaniline) attracted large attention because of valuable properties, including simple, reversible and unique doping–dedoping chemistry, stable electrical conduction mechanisms, high environmental stability and ease of synthesis.^[127,128] PAni reacts with a wide range of analytes and is very suitable for ammonia detection.^[129,130] Recently an electrohydrodynamic jet printing technique was employed to print PAni into flexible and rigid chemiresistive sensors arrays demonstrating ammonia detection at ppm level.^[131] A common limitation in organic/polymeric gas sensors concerns

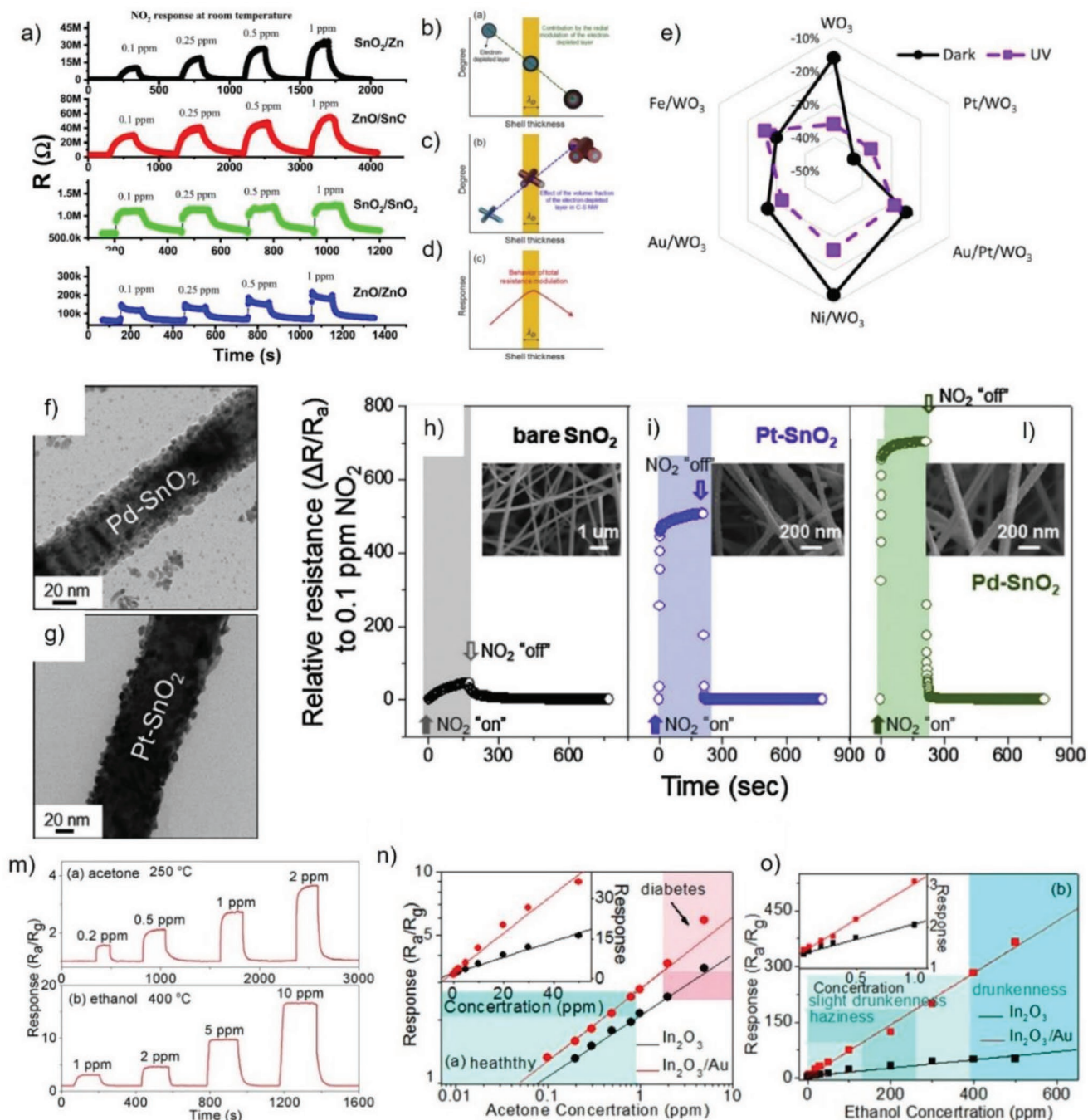


Figure 4. a) Room temperature dynamic response curves to different concentrations of NO₂ gas for SnO₂/ZnO and ZnO/SnO₂ heterojunctions and the SnO₂/SnO₂ and ZnO/ZnO homojunctions (from top to bottom) (reproduced with permission.^[106] Copyright 2021, Elsevier B.V.); b–d) contributions to ZnO–SnO₂ core–shell NWs gas response by radial modulation (shell thickness), shell volume fraction, and shell thickness, respectively (reproduced with permission.^[107] Copyright 2020, Elsevier B.V.); e) radar plot of the sensors response to 5 ppm CH₂O under dark (black circles) and UV light irradiation (violet squares) (reproduced with permission.^[124] Copyright 2020, Elsevier B.V.); f,g) TEM images of Pd- and Pt- functionalized SnO₂ NWs; h–l) 300 °C response curves to 0.1 ppm NO₂ for bare, Pt-functionalized and Pd-functionalized SnO₂ NWs, respectively (reproduced with permission.^[111] Copyright 2020, Elsevier B.V.); m–o) dynamic responses of m) In₂O₃/Au NRs and pure In₂O₃ gas sensor to different acetone concentrations at 250 °C and ethanol concentrations at 400 °C; n) In₂O₃/Au NRs and pure In₂O₃ gas sensors response curves to different acetone concentrations at 250 °C and o) ethanol concentrations (0.05–650 ppm) at 400 °C (reproduced with permission.^[125] Copyright 2015, Springer Nature).

their humidity susceptibility and poor recovery. Indeed, despite avoiding annealing steps is typically preferable, this procedure still remains a reliable strategy to desorb gas analyte and restore

pristine sensing abilities. In this respect, Yu and co-workers proposed the exploitation of “ion-in-conjugation” to achieve organic sensors operating at 100 °C and 70% relative humidity

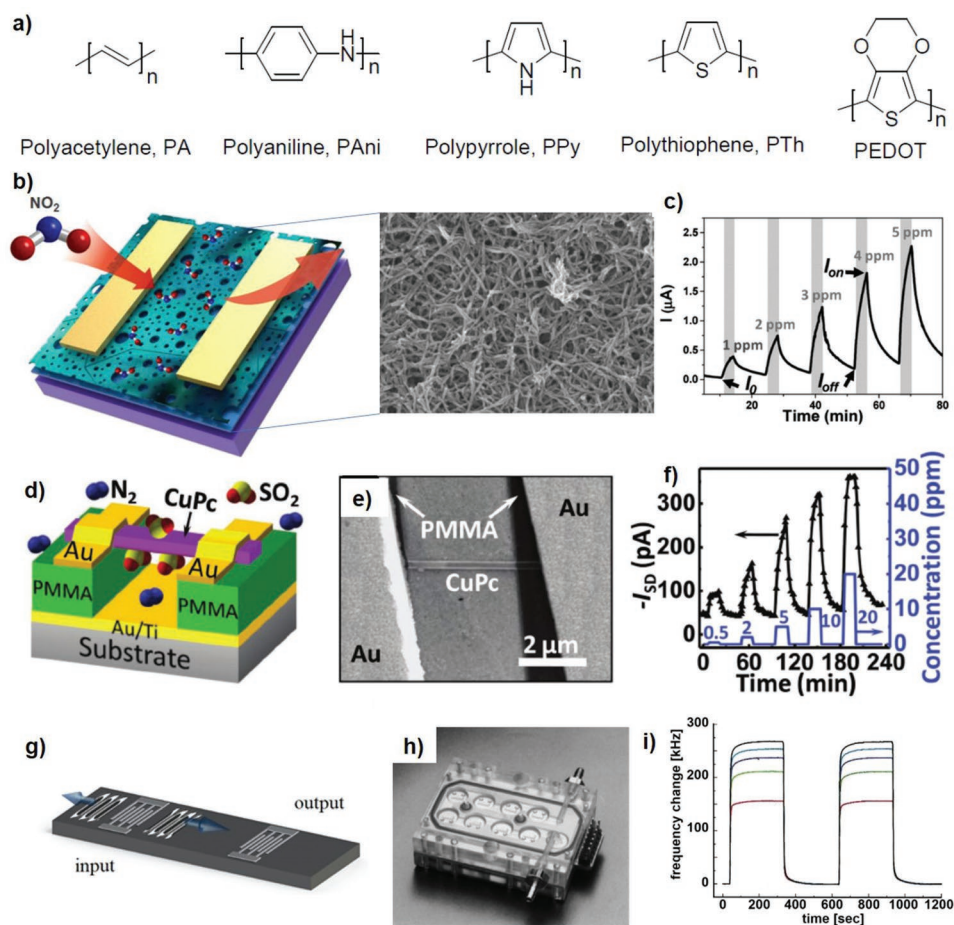


Figure 5. a) Main conducting polymers adopted in gas sensing (adapted with permission.^[12] Copyright 2007, MDPI); b) schematics of an organic field effect transistor and conducting PAni nanofibers film as active material for gas sensing (adapted with permission.^[173] Copyright 2021, Taylor & Francis Group); c) dynamic response of a 6,13-bis(triisopropylsilylethynyl)pentacene/para-sexiphenyl film based chemiresistor to NO₂ under 5 V bias (adapted with permission.^[141] Copyright 2017, John Wiley & Sons); d,e) schematic and SEM images of a gas sensor FETs based on a CuPc nanowire and f) real-time current change for increasing SO₂ concentrations (adapted with permission.^[133] Copyright 2013, John Wiley & Sons); g) schematics of a SAW sensor; h) picture of a SAW-based sensor array and i) frequency shifts of a SAW-based sensor sampling toluene levels (reproduced with permission.^[161] Copyright 2000, Elsevier B.V.).

with almost complete recovery and detection level down to (hundreds of) ppb range.^[132]

Besides polymers, conductive organic compounds made by the aggregation of molecular units show sensitive properties that can be exploited to prepare a variety of different gas sensors. Among them, pyrrolic macrocycles are made by a large aromatic system consisting of pyrrole units that can complex a metal ion at its center and can be further decorated with additional functional groups. The combination of these elements (aromatic ring, metal ion, and peripheral compound) determines the properties of the sensor. Thus, they are a sort of molecular platform whose sensitivity and selectivity can be modified by minimal changes of the molecular receptor structure. Porphyrins, corroles, and phthalocyanines are the most widely investigated members of the family. Solid state films of phthalocyanines show a semiconductor character and they have been used for organic electronics. Recently, Shaymurat et al. reported a gas sensor with sub-ppm sensitivity based on a copper-phthalocyanine (CoPc) single crystalline nanowire

organic field effect transistors (OFETs) (Figure 5d–f).^[133] Also conductive polymers were employed to implement gas sensors in the form of OFETs^[12,134–138] (Figure 5b). In this configuration, the active material conductivity is tuned by the gate bias and, when a constant source–drain voltage is applied, the exposure to gas analytes modulates the current flow^[139,140] as a result of carrier accumulation/depletion in the conducting channel resulting in a current increase/decrease. An example of a typical response is reported in Figure 5c in the case of a 6,13-bis(triisopropylsilylethynyl)pentacene/para-sexiphenyl film based chemiresistor detecting NO₂ under 5 V bias.^[141] Comparing organic FET devices with chemiresistors, the sensitivity can be improved at the cost of a more complex architecture. An often-observed drawback in many OFET gas sensors is a triangular shape of the response curve due to an absence of saturation (Figure 5c), which can be ascribed to the changing carrier density. An OFETs-based electronic nose was used to monitor chicken meat spoilage.^[142] In general, the dielectric layer/materials play an important role in determining the overall device

response and this aspect triggered FET research on novel dielectric (e.g., high k) materials for electronic applications and dielectric modulation for sensing.^[143–147]

2.2.2. Non-Conductive Organic Compounds

The main advantage of chemiresistors and field effect devices is in the low-complexity of the related front-end electronics and in their ready integration with microelectronics.^[3] However, only a limited portion of chemically sensitive organic compounds is sufficiently conductive. This is the case of those molecular structures, such as calixarenes and cavitands, characterized by cavities of molecular dimensions that can implement the molecular recognition.^[148] In these molecules the shape selection operated by the cavity is complemented by additional interactions, for example, hydrogen bond or π - π , that increases the sensitivity toward specific molecules. Although non-conductive, cavitands can be arranged as lateral groups of conductive polymers. This approach has been demonstrated with a tungsten capped calixarene moiety. Electrochemical polymerization of monomer units led to a conductive polymer that show a remarkable sensitivity to methane.^[149] However, besides to this approach, cavitands have mostly been used with non-conductive sensors.

When using non-conductive sensing layer, an efficient alternative to chemoresistors is offered by piezoelectric transducers which include QCM and SAW sensors, both based on mechanical oscillations and changes in the propagating wave (e.g., resonance frequency, phase, or amplitude) correlated with surface modifications due to adsorbed mass (or morphology changes) (Figure 5g–i).^[150–155] These devices exploit the relationship between oscillation frequency and mass, so that the change of mass, due to the absorption of airborne molecules, changes the resonance frequency. The sensitivity of these devices depends on the resonance frequency which is of the order of 10–30 MHz for QCM and above 100 MHz for SAW. SAW and QCM have been investigated in gas sensing applications from the 80's, and are still subject of intense study either in the form of SAW delay lines or resonators.^[126,156–163] For their implementation, interdigitated structures are fabricated on piezoelectric substrates (e.g., quartz) as transmitters and receivers (Figure 5g). As an example, Rapp et al. reported SAW-based sensor arrays able to sample toluene levels (Figure 5h,i).^[161] SAW sensors have important advantages, including low cost, ultra-high sensitivity, superior response time, small size, wireless mode, planar structure, excellent selectivity, fast response and linearity.^[164] For these reasons, different attempts have been made to build a compact gas sensing system using SAW technologies. On the other hand, QCMs because of the low frequency require a simple electronic interface and the frequency measurement ensures a high resolution. Thus, even if their mass sensitivity is smaller than in the SAW case, the chemical sensitivity is sufficiently large to enable, for instance, disease diagnosis from the detection of volatile molecules.^[9] On the other hand, mass transducers are intrinsically non-selective. This means that their signal is contributed by any mass change in the sensitive material irrespective of the involved interaction.^[165] However, selective sensitive materials are designed in order to emphasize

few interactions with respect to the others. This is the case of cavitands where synergistic CH- π , π - π , and steric interactions confer the desired selectivity. As an example, quinoxaline cavitands designed to detect aromatic and chlorinated vapors, when used to functionalize QCM sensors turn out to be also sensitive to acetone, acetonitrile and methanol.^[166] This finding evidences that mass transducers are more suitable to be used as sensor array elements in electronic nose applications.^[167]

Optical read-out offers another excellent alternative for the design of gas sensor, in the case of non-conductive sensing layer by monitoring changes in absorption (ultraviolet, visible, and infrared), reflection, refractive index or surface plasmon resonances (SPRs). In this respect, cavitands can be chemically modified to include chromogenic group that can signal the adsorption of volatile compounds with a change of absorbance spectra. This method was used for the detection of electron donor species, for example, ammonia and amines, where the adsorption of molecules to the cavitand is complemented by the deprotonation of the chromogenic group and the consequent change of color.^[168] However, it is worth mentioning here that other chemical materials, such as porphyrins and corroles show remarkable optical properties that are exploited for gas sensing.^[169] Furthermore, polyaniline-based optical sensors were also developed to detect gas analytes (e.g., ammonia) through refractive index sensing based on changes in SPR typically via reflectance measurements.^[170] Optical sensors are daily adopted in environmental quality control such as in cities, but today research focuses strong attention on other transduction principles such as chemiresistors also because of a reduced complexity of detecting systems. Recently, optical low-cost CO₂ sensors were reported in the form of polymer-coated fiber Bragg grating.^[171] The emergence of colloidal lithography then offers new opportunities for the low cost fabrication of localized SPR sensors.^[172]

2.2.3. Molecular Imprinted Polymers

Molecular imprinted polymers (MIP) are synthetic molecular structures mimicking the natural key–lock principle characteristic of antigen–antibody interaction.^[174] The MIP technique consists in the polymerization of monomers in the presence of a target molecule, which acts as a template during the synthesis of the polymer.^[175] Successively, the template molecules are removed from the polymeric matrix, leaving cavities of specific size, shape and functionality complementary to a target molecule (Figure 6a).

Compared with antibodies, MIPs are easy to prepare, reusable, and resistant to chemical and physical stresses. MIP sensors have been developed for detecting different analytes from environmental toxins to drug molecules, from nerve gas agents and explosives to pollutants.^[175,176] Moreover, molecular imprinted sensors have the advantages to be employable even in harsh conditions, including high temperature and pressure, and the presence of organic solvent and metal ions.

Specifically, in gas sensing field, Liu et al. realized a series of sensors, based on molecularly imprinted nanoparticles mixed at a perovskite-type oxide (LaFeO₃) doped with Ag, for selective detection of VOCs, such as formaldehyde, benzene, acetone

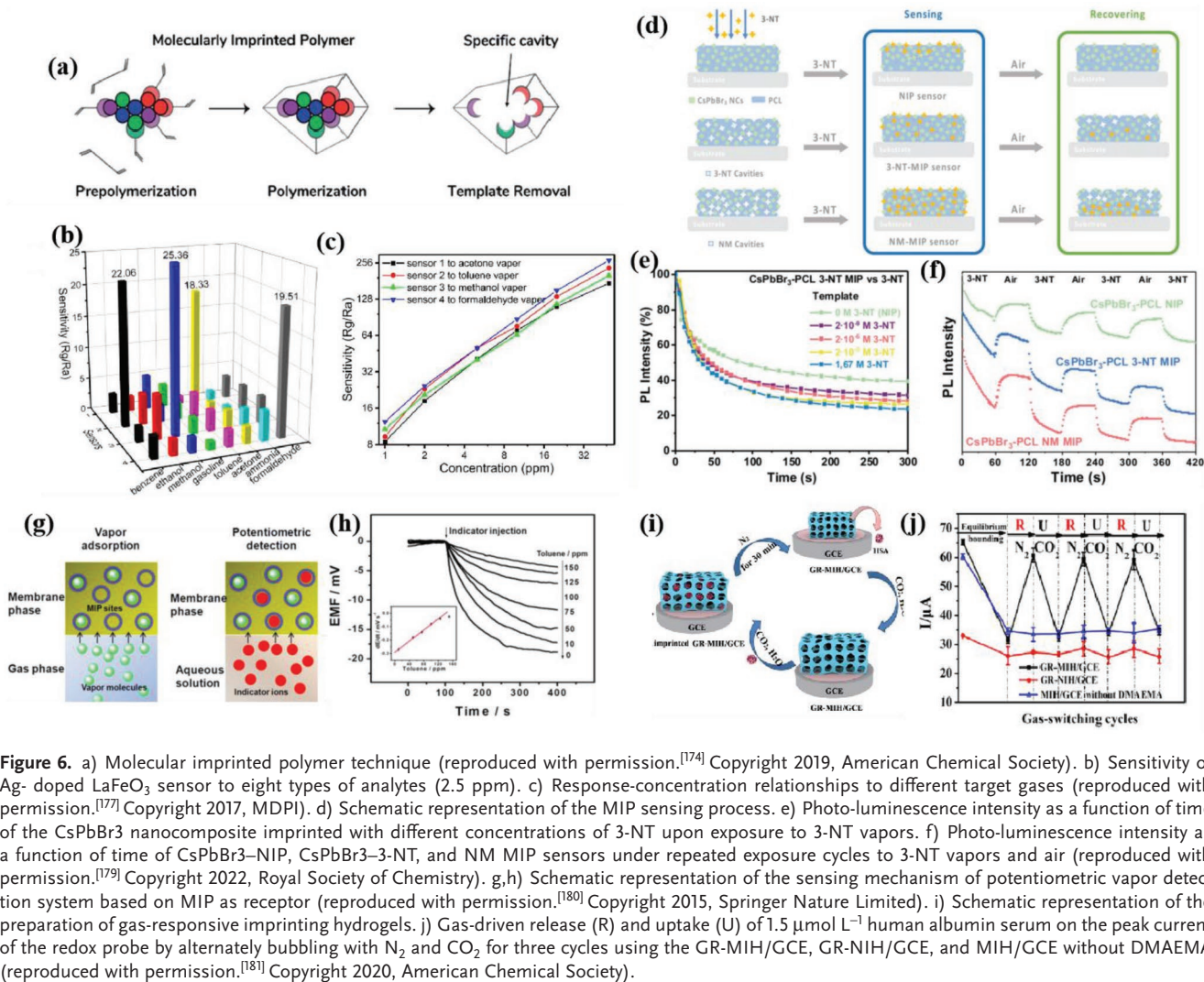


Figure 6. a) Molecularly imprinted polymer technique (reproduced with permission.^[174] Copyright 2019, American Chemical Society). b) Sensitivity of Ag-doped LaFeO₃ sensor to eight types of analytes (2.5 ppm). c) Response-concentration relationships to different target gases (reproduced with permission.^[177] Copyright 2017, MDPI). d) Schematic representation of the MIP sensing process. e) Photo-luminescence intensity as a function of time of the CsPbBr₃ nanocomposite imprinted with different concentrations of 3-NT upon exposure to 3-NT vapors. f) Photo-luminescence intensity as a function of time of CsPbBr₃-NIP, CsPbBr₃-3-NT, and NM MIP sensors under repeated exposure cycles to 3-NT vapors and air (reproduced with permission.^[179] Copyright 2022, Royal Society of Chemistry). g, h) Schematic representation of the sensing mechanism of potentiometric vapor detection system based on MIP as receptor (reproduced with permission.^[180] Copyright 2015, Springer Nature Limited). i) Schematic representation of the preparation of gas-responsive imprinting hydrogels. j) Gas-driven release (R) and uptake (U) of 1.5 μmol L⁻¹ human albumin serum on the peak current of the redox probe by alternately bubbling with N₂ and CO₂ for three cycles using the GR-MIH/GCE, GR-NIH/GCE, and MIH/GCE without DMAEMA (reproduced with permission.^[181] Copyright 2020, American Chemical Society).

and methanol (Figure 6b,c).^[177] Tang et al. exploited electropolymerization to cover TiO₂ nanotube array/Ti sheet with a MIP layer for selectively detecting formaldehyde in the ppm range at room temperature.^[178] For more details on the use of composite materials in gas sensing see Section 2.3.2.

In ref. [179], a solid-state luminescent gas sensor has been developed embedding a nanocomposite of CsPbBr₃ nanocrystals (NCs) in a MIP and using 3-nitrotoluene (3-NT) and nitromethane (NM) as template molecules to detect the presence of explosive markers such as 3-NT (Figure 6d–f). In particular, the authors showed that the photoluminescence (PL) intensity decreases significantly when the sensor is exposed to 3-NT for 60 s and recovers the PL of ≈83%, ≈78% and ≈72%, respectively, for NIP, 3-NT MIP and NM MIP when exposed to airflow.

Moreover, in ref. [180], a potentiometric sensing system based on a MIP was developed for the first time for detection of chemical vapors. Specifically, a MIP was integrated into an ion-selective electrode (ISE) membrane and used as the receptor for selective adsorption of the analyte vapor from the gas phase. In these systems, after vapor adsorption process, an indicator

ion with a composition/shape similar to that of the vapor molecule was exploited to point out the variation in the MIP binding sites in the membrane induced by the molecular recognition of the vapor (Figure 6g). The potential response of the MIP-based ion-selective electrode to the indicator ions decreases due to the decrease of available recognition sites caused by vapor adsorption. The proposed gas sensor was used to detect volatile toluene in the gas phase down to parts per million levels.

In ref. [181], gas-responsive imprinting hydrogels (GR-MIHs) were realized by combining N,N'-dimethylaminoethyl methacrylate gas-sensitive monomers (DMAEMA), N,N'-methylenebis(acrylamide) cross-linkers, and human serum albumin (HSA) template proteins by means of a free radical polymerization (Figure 6i). The GR-MIHs showed a reversible gas-responsive response after N₂/CO₂ exchange. The authors exploited this property for sensing applications, fabricating a CO₂-responsive imprinted biosensor on the surface of a glassy carbon electrode (GCE). In addition, the GR-MIH/GCE (Figure 6j) demonstrated an ability to uptake and release human serum albumin (HSA) under alternately flowing N₂ and CO₂.

2.3. Carbon Based, 2D, and Composite Materials

2.3.1. Carbon Nanotubes, Graphene, and 2D Materials

Several forms of carbon materials have been exploited for gas sensors, often in combination with other sensing layers. For this reason, they are described in this section along with composite materials.

Carbon black and carbon nanofibers have been used years ago to prepare chemiresistors with non-conductive polymers.^[182] However, among carbon materials, graphene and nanotubes present higher control of their surface chemistry.^[183] Since their introduction, carbon nanotubes (CNT) have been used to prepare chemiresistors and field effect devices for gas sensing purposes.^[184–186] Both physisorption and chemisorption can be involved in the process with associated electron transfer between the analyte and the sensing material. Gas analytes detected with CNT sensors include H_2O_2 , NO_2 , NH_3 , CH_4 , C_2H_5OH , CO , H_2 , H_2S , chlorine, and trinitrotoluene (TNT).^[186] The chemical sensitivity of CNT is exploited not only to detect gases but also to modify the CNT surface with functional groups to extend the sensitivity and selectivity. Further examples include sensors for VOCs based on CNT functionalized with porphyrins,^[187–189] DNA strands, cavitands,^[190] and nanoparticles.^[191–193] Disadvantages in using CNTs concern the expensive synthesis and risks associated to environmental release.

2D materials became very relevant after introduction of suitable techniques to produce graphene.^[194] Soon after, they attracted also interest for sensing applications.^[195,196] Within the gas sensor field, one of the first attempts of using graphene

dates in 2007 by Novoselov's group.^[197] Graphene (Figure 7a) shows molecular reactions similar to large-diameter carbon nanotubes but exhibits significantly lower noise levels. Pristine graphene-based gas sensors were reported in literature in the form of chemiresistors and transistors.^[198–202] However, because intrinsic graphene has no dangling bonds on its surface, graphene is more typically combined with polymers or functionalized with metals to enhance the chemisorption in gas sensor applications.

Reduced graphene oxide (rGO) was even more used than graphene. For example in ref. [203], a reduced graphene oxide (rGO)-based FET sensor with repeatable 100 ppm sensitivity to NO_2 was reported. In this case, annealing was employed to reduce the GO, make it more conductive and introduce reactive sites on the surface. More in detail, thermal treatments can be responsible of the oxygen functional groups removal from GO, and, as a result, the material recovers graphitic regions, making GO more conductive. These formed graphitic carbon atoms can result in active sites for gas analytes adsorption.^[203] Graphene oxide has also been adopted in the design and synthesis of hierarchical porous nanosheets, where the GO flakes act as scaffolds, resulting in enhanced sensing properties (Figure 7c).

Graphene and graphene oxide have been often mixed to other components to implement gas sensors, for example, in combination with metal-oxides (such as SnO_2 ,^[204–206] WO_3 ,^[207,208] TiO_2 ,^[209,210] metal oxide nanoparticles^[211] as well as ferromagnetic Fe_2O_3 nanoparticles^[212–216]), nitrides,^[217,218] PMMA nanocomposites,^[219] polyaniline,^[220] and 2D transition metal dichalcogenides.^[221–224] Due to its mechanical properties, graphene in blend with polymers was adopted to produce textile-integrated gas sensors.^[225,226] In another study, metal oxide-modified

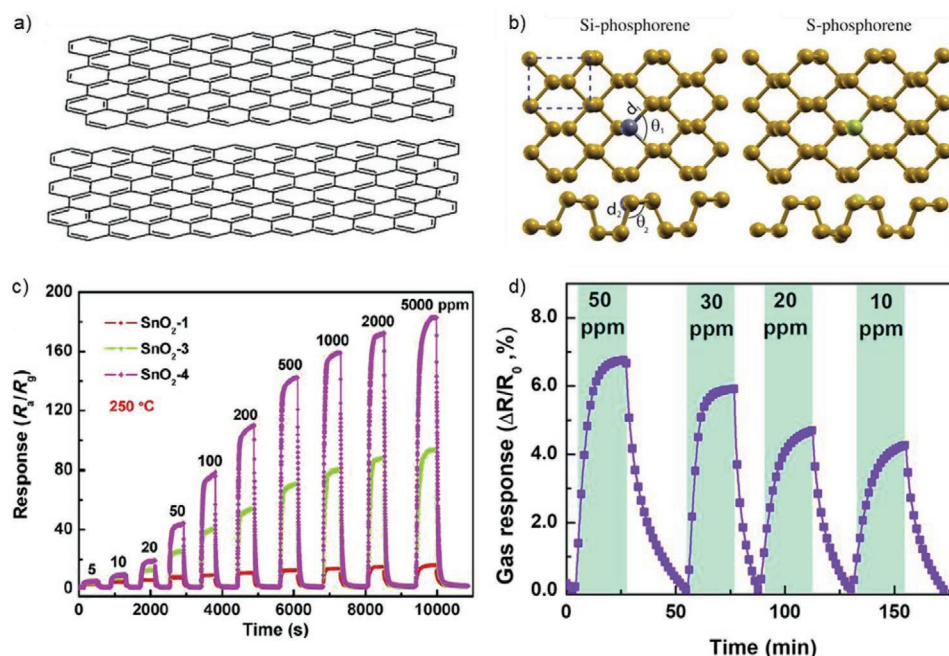


Figure 7. a) Graphene layers (adapted with permission.^[195] Copyright 2012, Elsevier B.V.); b) Si- and S-doped phosphorene structures (adapted with permission.^[231] Copyright 2019, Elsevier B.V.); c) hierarchical SnO_2 based sensors response to 5–5000 ppm ethanol, with different amounts of GO powder in the preparation (0.5, 3.0, and 5.0 mg, respectively) (reproduced with permission.^[206] Copyright 2018, Elsevier B.V.); d) $Ti_3C_2T_x$ MXene/graphene hybrid fibers-based chemiresistor response to NH_3 (reproduced with permission.^[237] Copyright 2020, American Chemical Society).

graphene-based sensor array were combined with neural network models.^[227] Notably, selective ppb-level detection of NO₂ was reached in a gas sensor based on graphene combined with SnO₂-boron nitride nanotubes.^[228] However, the role of graphene in determining the gas sensor performances is not completely clear.

Within 2D materials, phosphorene (a mono- or few-layer black phosphorus) is expected to exhibit excellent adsorption properties for CO, CO₂, NH₃, NO, and NO₂ according to theoretical studies.^[229,230] These studies predict superior sensing performance that could surpass alternative 2D materials such as graphene. In ref. [231], another theoretical study reports that Si- and S-phosphorene doping can improve sensitivity in these sensors (Figure 7b). Other 2D materials have been also investigated in gas sensing, such as transition metal dichalcogenides, which are reviewed in ref. [232]. Really promising results have been reported, such as the chemically exfoliated MoS₂ flakes-based sensor by Donarelli et al. that have a LOD of 20 ppb for NO₂ gas.^[233]

A new class of 2D transition metal carbides or carbonitrides (MXenes) recently showed exceptional and promising properties in terms of sensitivity and selectivity. In ref. [234], an acetone sensor with 0.5 ppm LOD has been reported. In ref. [235], a hybrid active layer made of PANi and MXene resulted in very good selectivity and sensitivity to ammonia detection while in ref. [236], Schottky barriers formed in TiO₂ and Ti₃C₂ MXene films led to a sensor high responsive to NO₂. In ref. [237], Ti₃C₂T_x MXene/Graphene hybrid fibers-based chemiresistor response to NH₃ was investigated, finding very good responses to the gas analyte (Figure 7d).

2.3.2. Composites

Gas sensors based on organic compounds and polymers continue to improve their performance, but their sensitivity and stability remain too constrained to their high affinity toward VOCs and the moisture of an environment. On the other hand, gas sensors made from inorganic materials and metal oxides show higher sensitivity with respect to organic gas sensors as a result of a variation in oxygen stoichiometry and changes in charge carrier density within the active region, but they typically require high temperatures, leading to oxidation of analytes and to baseline drifts.^[14] Carbon based materials instead are typically used in combination with other compounds to increase processability and performance.

A method to combine the advantages of different active layers resides indeed in designing composite materials^[6,19] with unique ensembles of properties. For example, organic–inorganic composites can overcome issues related to low conductivity and poor stability of organic materials and the limiting operation condition (high temperatures) in the case of inorganic metal oxides, then improving overall stability, selectivity and sensitivity, reducing operation temperatures and response time and also providing new characteristics such as flexible mechanical properties.^[238]

In general, composite materials can consist of: i) an organic phase, typically in the form of conductive polymers; ii) an inorganic phase made of metal oxides, semiconductors and metal

nanoparticles; and iii) carbon-based or 2D materials. The different combinations reported in literature (Figure 8a) include metal oxides with semiconductors,^[43] polymers,^[239,240] metal-organic frameworks^[241] or carbon-based materials^[205,207,242–244] as well as polymers with carbon-based materials^[245] or 2D materials.^[235] An application-specific tuning of the composites hybrid properties can be achieved by varying synthetic routes and precursors, composition and morphological/interfacial characteristics.^[14]

Because of the interactions between the constituent materials, composites can present more complex and, in different cases, not completely understood sensing mechanisms. In many cases, however, the sensing mechanism of organic–inorganic composites can be described as a gas-induced modification in the width of the depletion region at the interface between organic p-type materials and n-type oxides. This active region at the interface can be considered as a p-n junction whose resistance is modulated by gas exposure.^[14]

The improved performance with composites can be ascribed to a combination of effects, in relation to the particular configuration/mixture. The sensors can benefit from larger specific surface areas, more active and different interaction-sites, ultrahigh porosities, and strong gas adsorption capacity.^[241] The formation of heterojunctions between the integrated materials turns out to have a remarkable impact on sensitivity and allows a drastic reduction in the response time, particularly with graphene-based composites.^[244] Improved gas sensor capabilities can also be achieved by engineering the interaction sites. For example, the combination of polyaniline with carbon nanotubes increases chemical interaction between pristine material and gases by promoting their adsorption through physical dipole–(induced) dipole interactions, which may uncoil the polymer chains and decrease the hopping distance for the charge carriers.^[246] An increased stability in the environment has been also reported, with a reduced influence of humidity on the response when the active sites for water adsorption are occupied in the composite as a result of intermolecular hydrogen bonds between the two active materials.^[235]

As specific examples, in Figure 8b,c the dynamic response curves of QCM sensors to formaldehyde vapors are reported in the case of three different active layers (sole SnO₂ nanofibers [NFs], sole polydopamine and SnO₂ NFs/PDA composites), that indicate a clear improvement in the composite sensor performances which result in a significant increase in the frequency shift ascribed to hydrogen bonding of the analyte and aldehyde ammonia Schiff base interactions.^[239] In the work from Gai et al., a ternary composite was employed by modifying the surface of carbon nanotubes through pyrrole polymerization and Cobalt phthalocyanines (CoPc) conjugation via π - π interactions.^[247] The resulting sensor exhibited ultrafast response (12 s) to NH₃ by exploiting the 3D MCNT network and the additional sensing capability of CoPc (LOD 11 ppb, stability over 60 days and humidity resistance). Composite materials were also reported to present “p- to n-” type behavior transition observed in CNT/ZnO composites by varying the operating temperature (Figure 8d–f).^[242] This response was attributed to the switching of the most responding sensing component (from CNT to ZnO).

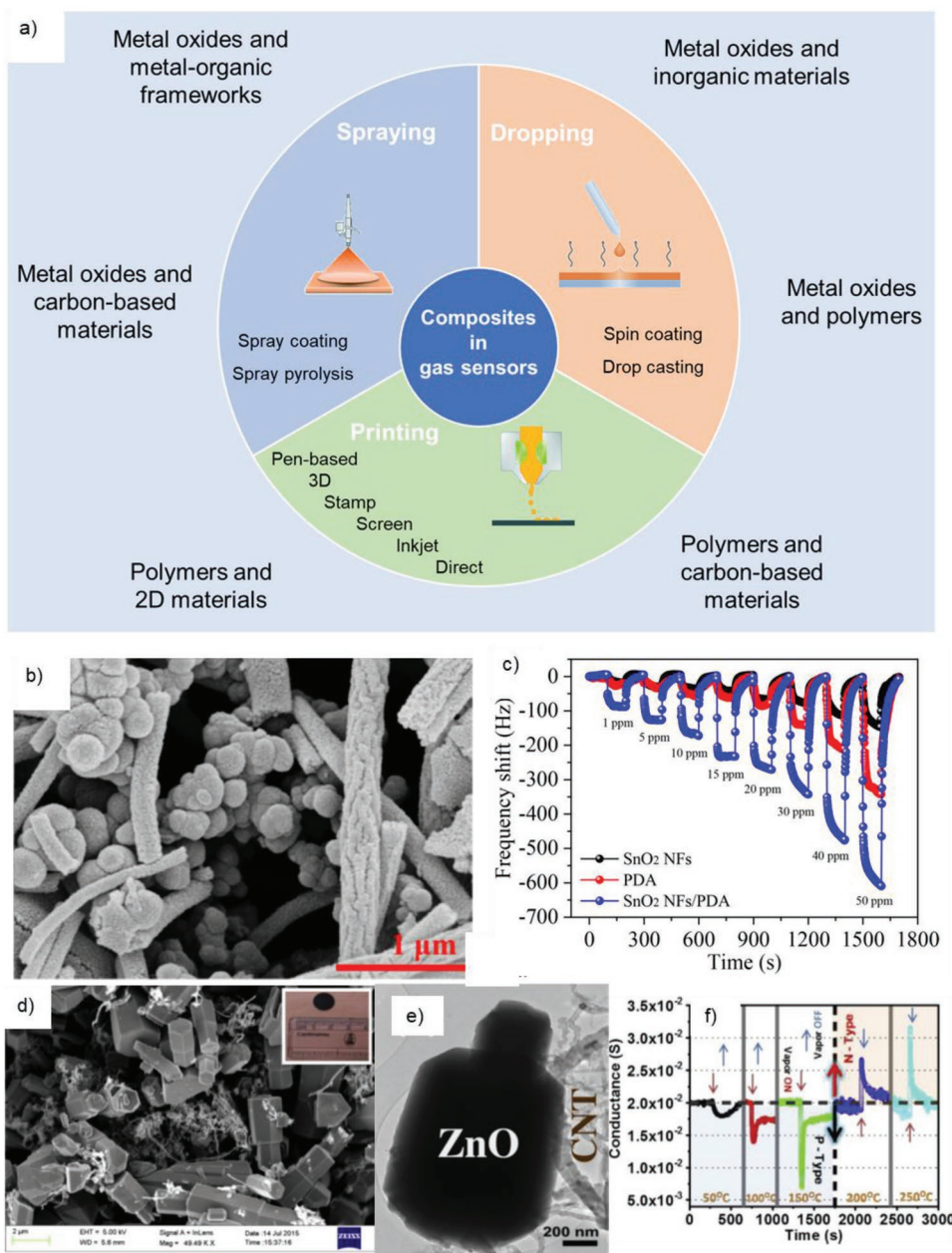


Figure 8. a) Composite materials in gas sensors and related deposition techniques; b) SEM images of SnO₂ nanofibers/polydopamine (PDA) composite; c) dynamic response curves of QCM sensors based on SnO₂ nanofibers, polydopamine, and SnO₂ nanofibers/polydopamine to formaldehyde vapors at 25 °C (reproduced with permission.^[239] Copyright 2021, Elsevier B.V.). d) FESEM image of CNT/ZnO composite proposed in ref. [242] presenting a switching of gas adsorption process with p- to n-type transition, depending on the working temperature; (in the inset a pellet with 1 cm diameter); e) TEM image detail of ZnO microparticles attached with CNTs; f) conductance versus time under exposure to 25 ppm methanol at different operating temperature. For temperatures above 150 °C, the material behavior switches from p-type to n-type (reproduced with permission.^[242] Copyright 2021, Elsevier B.V.).

3. From Traditional to Novel Applications of Gas Sensor Technologies

3.1. Commercial Sensors and Electronic Noses

Today various traditional gas sensors are available on the market and their use spreads in numerous sectors. The most common devices are based on optical transducers or chemiresistors. This last class often employs metal-oxides active layers and presents

advantages in terms of miniaturization and long life. **Table 1** summarizes the main transduction methods employed to implement gas sensors with their specific advantages and limiting factors.

The integration of gas sensors in electronic noses (e-noses) is a major technological target to offer generic devices suitable for various applications. The ambition is to mimic human olfaction in order to detect complex patterns of gases and recognize the unique fingerprint associated to a substance/environment/condition. First attempts to develop olfaction devices can be ascribed

Table 1. Transduction methods employed for gas sensing, with details on their working principle, advantages and limiting factors.

Transducer	Working principle	Advantages	Limiting factors
Optical sensors	Changes in optical absorption, emission, or refractive index	Fast response time (below 1 s), minimal drift and high gas specificity and sensitivity	Need of excitation sources and detection devices, lower portability, expensive
Chemiresistors	Changes in impedance	Suitability for miniaturization and arrays, high sensitivity	Sensitive to humidity, high working temperature and power consumption (if based on metal oxides), unstable in the atmosphere and long recovery times (if based on polymers)
Transistors and diodes	Changes in the flowing current under a fixed applied voltage	Presence of additional parameters for measurements if compared to chemiresistors, low operating voltages, low operating temperatures, large-scale manufacturing	Absence of unified working mechanism model; need of improvements for OFET sensors; more complex with respect to other devices
Piezoelectric sensors	Changes in acoustic waves signal amplitude/resonant frequency	High sensitivity, superior response time, good response time, small size	Sensitive to external interferences (e.g., temperature) as well as to internal defects
Catalytic sensors	Temperature variations due to gas analyte combustion	Low sensitivity to humidity, low cost, fast response and recovery time	Low sensitivity, low selectivity

to Moncrieff in 1961 and a sort of electronic nose was developed by Wilkens, Hatman and Buck in 1964 when the knowledge of physiology of olfaction was still limited.^[248] Thus, the real development of electronic noses began only after the finding that the olfactory receptors are not strictly speaking selective, but rather they can detect more than one compound albeit with different affinity.^[249] Thanks to this property, a single odorant is converted into a pattern of receptors signals. In this way, with a limited repertoire of receptors (e.g., about 300 in humans), it is possible to easily detect up to billions of different stimuli.^[250] In 1982 for the first time an array of cross-selective metal oxide gas sensors was conceived as a sort of artificial olfaction system.^[251]

However, making an electronic nose is a challenging task, often demanding compromises during design. For example, some very specific human receptors are based on irreversible interactions with analytes, such disposable receptors are internalized after each detection.^[252] Other olfactory receptors have instead a lifetime of a few weeks.^[11] On the other hand, the general lifetime of artificial sensors must be much longer for practical applications. Using an array of sensors responding in a different manner to a fixed stimulus, it is possible to cross data and obtain information on the environmental composition.^[9,11] However, emulating olfaction means reaching both high sensitivity for odors and high discrimination between them, which are still subjects of intense research. Furthermore, suitable methods for data analysis are required to achieve odor recognition.

From a biological point of view, odors recognition is achieved by comparing the signal of millions of nose receptors with analytical support from the brain.^[11,20,253,254] Technologically, a multi-sensor array is used in combination with an information-processing unit, a software with digital pattern-recognition algorithms and a reference-library database to provide the composition of an analyte mixture, also referred to as electronic analyte fingerprint. Today statistical methods and pattern identification strategies include Principal Component Analysis, Linear Discriminate Analysis, Partial Least Squares, Functional Discriminate Analysis, Cluster Analysis, Artificial Neural Network, Probabilistic Neural Network.^[255] Among them, Principal Component Analysis (PCA) reduces the dimensionality while

preserving most of the information by projecting the multi-dimensional data into a new coordinate system in order to maximize the variance and minimize the correlation between data.^[256,257] As an example, four different simulants of chemical warfare agents^[258] were discerned from data provided by four SAW sensors with different active layers (ZnO, TeO₂, SnO₂, and TiO₂) (**Figure 9**). In this case, PDA analysis led to define two principal components (PCA1 and PCA2) preserving most of the information (97%) because the variance of PCA1 and PCA2 are 82% and 15%, respectively.

Linear Discriminate Analysis (LDA) is another technique to lower the dimensional space and achieve pattern recognition by means of linear combinations of the measured variables.^[259] Discriminant functions are used to reveal data clusters by maximizing the classes distance associated to the within-classes variance. Comparisons between PCA and LDA are reported in refs. [260, 261], both indicating that LDA is more efficient than PCA. In general, PCA can be labelled as an “unsupervised” algorithm while LDA is “supervised”.^[261] In ref. [142], LDA has been used to lower a 4D matrix of data coming from four OFET transistors groups to detect meat spoilage. In ref. [262],

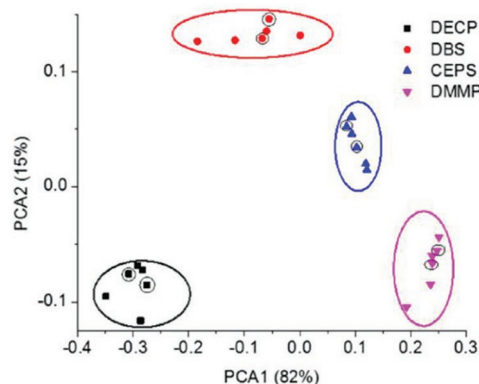


Figure 9. Example of PCA application for vapors discrimination using data from an array of SAW sensors (reproduced with permission.^[258] Copyright 2013, Elsevier B.V.).

both PCA and LDA are reported and decision tree (DT) and k-nearest neighbors (KNN) techniques are used for analytes classification.

In recent years, methods based on Artificial Neural Networks are gaining interest. These approaches are inspired by the biological neurons and are generally used in gas sensing to classify an unknown data set starting from well-defined clusters of data.

3.2. Safety, Industrial, and Environmental Monitoring

Gas sensing technologies have significant applications in safety, industrial, and environmental monitoring. In all cases, the urgency comes from the increasing levels of industrialization, urbanization, and pollution in different areas of the planet and the negative consequences on human health and biodiversity. Furthermore, these fields share both the need for on-field continuous/real-time measurements and a common set of target gas analytes.

Environmental monitoring has become a primary need for the global agenda targeting a sustainable growth.^[54,263] New user-friendly technologies are requested for the detection of particulate matter (PM) or hazardous gases (e.g., NO₂ levels) in the air as well as pollutants and microplastics in fresh waters or contaminants in/from industrial processes. Innovation is particularly necessary where low risk thresholds need to be detected to protect human health and the ecosystem. Calorimetric/thermometric sensors have been proposed for online pipeline inspection and high-temperature harsh environment but they generally present low selectivity and today are not widely investigated.^[264,265] In the last two decades, instead, semiconducting metal oxides devices have been widely used as sensors for hazardous gases,^[22] despite some limitations for explosive gases sensing because of their high working temperature. Nowadays, composite materials seem very suitable for sensitive devices in environmental applications.

Beyond monitoring on the (external) environment, the detection of environmentally hazardous gases and VOC concentrations in indoor domestic areas is also important (e.g., in realizing smart homes able to monitor the presence of a safe environment). For this purpose, the devices should be inexpensive, selective and suitable for real-time detection, user friendly operation, miniaturization and large-scale fabrication. Chemisensors (and in particular chemiresistors based on metal oxides and conductive polymers) well respond to these requirements.

In general, looking to increasing performances, organic-inorganic nanocomposites have been discussed to be among the best options to selectively discriminate the presence of hazardous pollutants in the air and in residential areas.^[14] For example PAni-MWCNT detectors permitted sensing of hydrocarbon vapors in the 200–1000 ppm range.^[245] In future, an increased use of nanomaterials (and their nanocomposites) in the sensing layers can be expected, as far as the production cost will decrease and/or the target application motivates a larger cost.

Table 2 summarizes some characteristics of most effective sensors (active layers and transducers) suitable for pollutant gases detection. As is clearly visible, composite and nanomaterials based sensors are the most performing in most cases. Limits of detection range from 50 ppt in NH₃ case to 7 ppm

in H₂ case. The innovation trend in term of sensing layer is clear in hydrogen detection, with recent reports focusing on the use of nano-heterostructures exploiting for example Pd catalytic properties.

3.3. Food Monitoring

Food monitoring is a major field for gas sensing application, especially in industrial processes and along the distribution chain. Indeed, the electronic discrimination of gases produced during food fabrication can help in the standardization process and quality control, but also to successively monitor their status and conservation as well as tracing their origin.^[255] In the near future, we can expect food quality to improve as the information related to food production and packaging increases, especially with the development of Internet of Things.^[283,284]

There are several gases involved in the food decomposition mechanisms,^[8] such as: H₂, CO, NO₂, O₂, H₂S, NH₃, CO₂, CH₄, H₂O, C₂H₅OH (ethanol), and the correlation between some VOCs and food spoilage has been widely studied in literature. Some examples are: NH₃, cadaverine and putrescine present in meat deterioration;^[285,286] H₂S and NH₃ associated to fish festering^[287,288] and fruit fermentation producing ethylene;^[289–291] milk fermentation bringing out gases such as 2-octanol, decane, 1-propanol and n-butanol.^[292] Furthermore, specific gases/aroma can be associated to food of different origin.

As a result, in the past years, electronic noses were developed for the milk/dairy industry to allow the detection of unspoiled and spoiled milk, the discrimination of different milk flavorings, and differentiation of milk collected from healthy and mastitis disease affected cows, including also bacterial contaminations and milk fermentation examination.^[292–297] Strong benefits can be achieved also for the wine industry with detection of different off-flavors in wines of different origin, classification of wines, and identification of French/Italian wines.^[298–300] In this respect, e-noses present significant advantages and have been also applied for the detection of aroma from green tea at different storage times, identification of optimum fermentation time for black tea, quality evaluation and classification of black tea,^[284,301–303] analysis of coffee samples,^[304] quality identification of rapid fermented fish,^[287,288] meat spoilage detection,^[285,286] freshness evaluation of leeks and bananas,^[305] and machine learning classification for cheese, liquor and edible oil samples.^[306] Various studies based on the involved gas analytes^[307] and reviews have been also published.^[308–310]

Colorimetric sensors were proposed (**Figure 10a**) as a user-friendly and a ready-to-use solution for everyday food consumption due to their easy read-out for the consumer.^[311,312] These kinds of sensors also evolved into colorimetric QR codes that can be read via smartphone (**Figure 10b**). However, colorimetric readout can be affected by uncertainties associated to user evaluation. For this reason, great part of the research focuses on electronic sensors. In **Figure 10c**, a smart packaging system for monitoring meat spoilage within its packaging is shown.^[286] In ref. [290], instead, sol-gel sensors working at room temperature were employed for fruit monitoring via e-noses with the target to minimize the food waste and maximize the fruit

Table 2. Some examples of pollutant gases, their health effects, guidelines and state-of-the-art gas sensor technologies for their detection according to literature.

Hazardous compound	Health effects	Guidelines	State-of-art gas sensors		
			Active material	Measured physical quantity	LOD
HCl	Short-term exposure: eye, nose, and respiratory tract irritation and inflammation and pulmonary edema in humans. Long-period exposure: gastritis, dermatitis, and photosensitization in workers. Dental discoloration and erosion. EPA has not classified hydrochloric acid for carcinogenicity. ^[266]	489 ppb (hyperplasia mucosa) ^[266]	Nanocomposite copolymers of aniline and formaldehyde synthesized with a metal complex of Fe–Al ^[267] (95:05)	Variation of DC electrochemical conductivity of active layer	0.2 ppm
NH ₃	Short-period exposure: immediate throat irritation; cough. Long-period exposure: laryngeal and pulmonary edema and bronchopneumonia, chronic bronchitis, and bronchiectasis. ^[268]	400 ppm irritation to 1700 ppm cough to 2400 ppm more severe symptoms ^[268]	PAni nanograins on TiO ₂ fiber surface ^[269]	Variation of RF electrochemical conductivity of active layer	50 ppt
H ₂ S	Short-term exposure: respiratory and ocular irritation, neurological effects; death may result as a consequence of respiratory failure. Long-term exposure: increased rate of spontaneous abortion. ^[271]	110 ppb (1-day) ^[272]	PANI-SWCNT ^[270]	FET transfer characteristics	50 ppb
			PAni-Au nanocomposite ^[273]	Chemiresistance variation	0.1 ppb
NO ₂	Eye, nasal, throat irritation and cough, bronchitis symptoms of asthmatic children ^[275]	100 ppb (1-hour), 20 ppb (1-day) ^[272]	Graphene-Cu ₂ O nanosheets ^[274]	Electric resistance variation	5 ppb
			Au-PVC nanocomposite electrode ^[276]	Cyclic voltammetry	50 ppb
NO	Pulmonary alterations with lesions of type I cells and cilia-bearing epithelial cells ^[277]	2 ppm (8-hour) ^[277]	Te nanotubes ^[96]	Chemiresistance variation	500 ppt
CO	Inhibits the transportation of oxygen in human blood, hypoxia. ^[275]	26 ppm (1-hour), 9 ppm ^[272]	Si nanowires ^[95]	Normalized resistance variation	500 ppb
H ₂	Non-toxic, explosive. ^[279]	10% in air ^[279]	PAni-Fe/Al (80/20) nanocomposite thin films ^[278]	Electric conductivity variation	0.06 ppm
			Pd/Cu NWs on SAW ^[126]	Transmission parameter variation	7 ppm
SO ₂	Short period exposure (up to 24-hour at concentration level <125 mg m ⁻³): reduction in mean forced expiratory volume over one second (FEV ₁), increase in specific airway resistance (sRAW), chronic obstructive pulmonary disease (COPD). ^[281]	175 ppb over 10 min ^[281]	VO ₂ nanobelts ^[280]	Chemiresistance variation	0.17 ppm
			Vanadium doped tin dioxide ^[282]	Resistance variation	<5 ppm

quality. In general, post-harvest maturation process is very relevant for modern food industry.^[289] In Figure 10d, results are reported from a study performed on “Golden Delicious” apples ethanol emissions to monitor the decomposition process.^[289] The PCA analysis in Figure 10e instead represents the results obtained from the comparison between BWL (white), TGO (green), and TBV (black) tea.^[284]

In terms of performances, the most performing layers for H₂, CO, NO₂, and H₂S, NH₃ were already discussed in the previous section and consist of nanomaterials and composites (see Table 2). For O₂, CO₂, and H₂O, no high performances are required due to their presence at high concentrations and presently available commercial sensors (mainly based on metal oxides) do not require relevant improvements. Concerning

ethanol (C₂H₅OH), the most performing sensors employ metal oxides nanomaterials or their composites, while CH₄ is better detected with metal oxides and their nanomaterials, with the possible on-chip integration of microfilters as a way to improve selectivity.^[313]

3.4. Volatilomics and Biomedical Diagnostics Applications

Metabolomics gained strong attention in diagnostics since it provides information about cellular processes and health status. The volatile fraction of the metabolome, called the volatilome, is particularly appealing because of the supposed simplicity of samples collection, the intrinsic non-invasiveness of

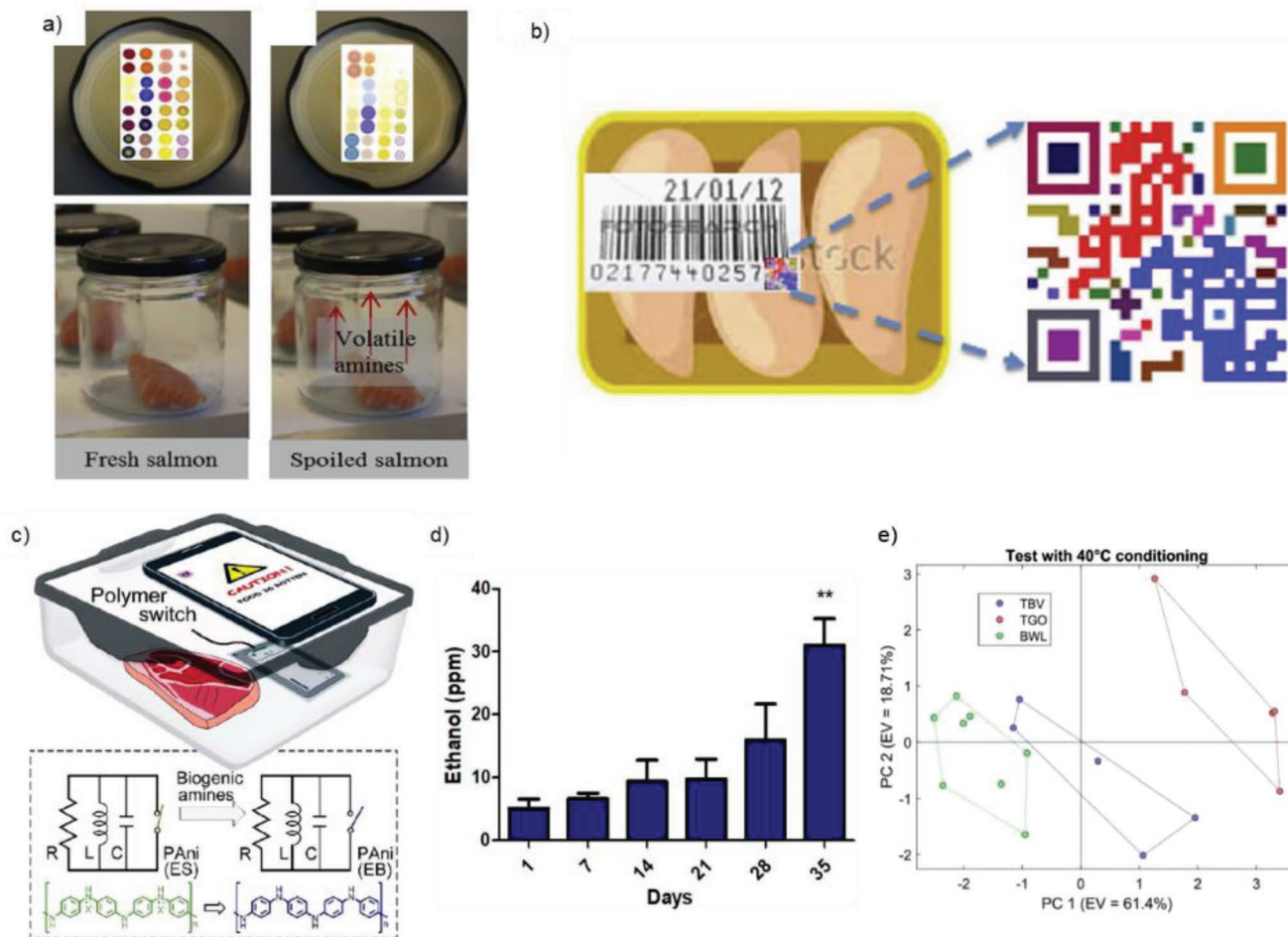


Figure 10. a) Colorimetric sensor array response at 0 and 24 h spoiling salmon (reproduced with permission.^[311] Copyright 2016, Elsevier B.V.); b) colorimetric QR-code for quantitative evaluation of food ageing and quality (reproduced with permission.^[314] Copyright 2017, Elsevier B.V.); c) wireless system based on polyaniline devices to monitor meat spoilage (reproduced with permission.^[286] Copyright 2018, American Chemical Society); d) ethanol concentrations emitted from apples during spoilage process (reproduced with permission.^[289] Copyright 2020, MDPI). e) PCA analysis representing the results obtained from the comparison between BWL (white), TGO (green), and TBV (black) tea (reproduced with permission.^[284] Copyright 2021, MDPI).

measurements and the wide availability of analytical methods. Studies show that patterns of VOCs are related to a vast range of phenomena observable *in vitro*, even at single cell level,^[315] and *in vivo*.^[316] Several instrumental techniques are available for the analysis of volatiles. Gas chromatograph and mass spectrometers provide a thorough analysis of the volatile composition. On the other hand, portable and easy to use instruments based on gas sensors are also becoming available in the form of electronic noses.^[9]

The human volatile is very complex. It contains about 2000 different compounds and all the major chemical families are represented. The largest diversity of compounds are found in breath.^[317] This abundance is due to the chemical and physical mechanisms that lead from the excretion of metabolites in cells and tissues, to their dilution in blood and finally to the exchange, in the lung, at the blood–air interface. Since the partition coefficients of each molecule is different, the abundance of compounds in breath is greatly variable. All organs can contribute to the VOCs collected in breath. Indeed, breath analysis

can detect cancer affecting not only lungs but also breast, colon, and prostate through an appropriate pattern of VOC biomarkers.^[10,318] An array of porphyrins-coated QCM sensors provided in 2003 is the first evidence that gas sensors can distinguish lung cancer from the analysis of breath.^[319] Furthermore these sensors were used to analyze VOCs from other bodily samples such as urines for kidney cancer^[320] and blood serum for COVID-19.^[321] Interesting results in breath analysis have been obtained with chemiresistors made of organically capped gold nanoparticles.^[322] These sensors showed brilliant results in diagnosing several diseases including lung cancer,^[6] colon cancer,^[323] and gastric cancer.^[324]

PCA techniques can largely help in data analysis.^[325–327] As an example, **Figure 11a** shows as a good classification can be achieved among exhaled breath from chronic kidney disease (CKD), diabetes mellitus (DM) and healthy subjects, obtained through an e-nose and PCA technique.^[327] In **Figure 11b–e**, the same pattern recognition technique was used to distinguish between diabetes, breast cancer, halitosis and healthy breath,

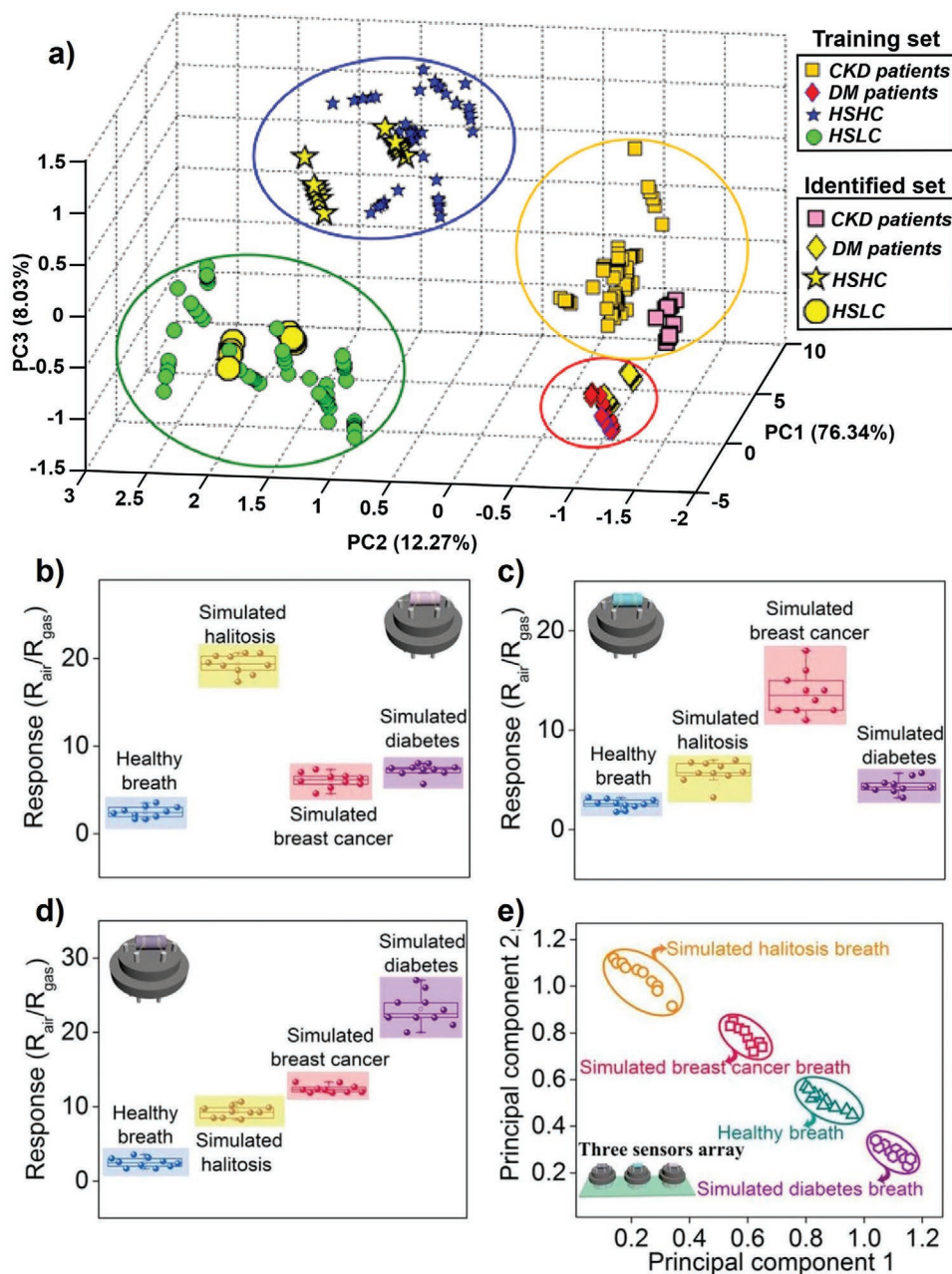


Figure 11. a) PCA on e-nose data to investigate exhaled breath of chronic kidney disease (CKD), diabetes mellitus (DM), and healthy subjects with high and low creatinine (HSHC and HSLC) (reproduced with permission.^[327] Copyright 2018, Elsevier B.V.); b–d) simulated breath (halitosis, breast cancer, and diabetes) sensing responses of Au-In₂O₃ nanowires, Ag-In₂O₃ nanowires, and Pt-In₂O₃ nanowires-based sensors, respectively. e) PCA and pattern recognition based on dataset from arrays made of Au-In₂O₃ NW sensors, Ag-In₂O₃ NW sensors, and Pt-In₂O₃ NW sensors (reproduced with permission.^[325] Copyright 2019, Royal Society of Chemistry).

by using sensors with active layers made of nanowires functionalized with different noble metal catalysts and capable of detecting levels of 50 ppb hydrogen sulfide, 8 ppb formaldehyde and 20 ppb acetone.^[325]

In biomedical applications, however, gas sensors with high sensitivity and selectivity are needed to detect very low (ppb and sub-ppb) concentrations of target gases associated to human pathologies (Figure 12) and, moreover, the human breath consists of a very complex mixture with a high humidity content

which set further difficulties. To avoid condensation, heating systems and breath delivery systems have been studied;^[328] moreover active materials providing humidity-independent gas sensors (e.g., based on NiO-loaded SnO₂) are today available in literature as suitable options for breath-based diagnostics.^[23]

An attempt to provide a correlation among VOCs content and some relevant human diseases is reported in Figure 13. In general, it seems not possible to find a specific marker for lung cancer, but a family of VOCs values are altered in the presence

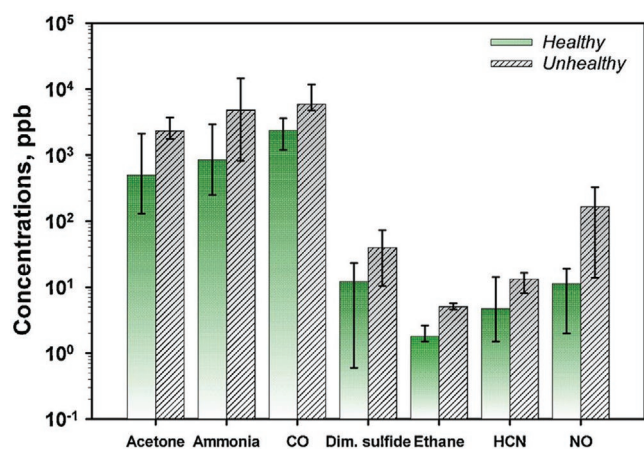


Figure 12. Proposed breath markers for different pathologies: diabetes, kidney disease, lung inflammation, liver disease, schizophrenia, bacterial infection, and asthma (reproduced with permission.^[328] Copyright 2015, Elsevier B.V.).

of this disease. In ref. [329], a list of VOCs of interest for lung cancer diagnosis is given including hexane, heptane, octane, nonane, decane, undecane, 1-methyl-2-pentylcyclopropane, isoprene2-methyl-1,3-butadiene, 2-methylpentane, methylcyclopentane, cyclohexane, 2-methylheptane, 2,2,4,6,6-pentamethylheptane, 2-methyloctane, 3-methyloctane, 3-methylnonane, 1-hexene, 1-heptene, 1-octene, benzene, trimethylbenzene, ethylbenzene, propylbenzene, toluene, o-toluidine2-amino-1-meth-

ylbenzene, m-toluidine 3-amino-1-methylbenzene, aniline, styrene, xylenes,2,3-dihydro-1-phenyl-4(1H)-quinazoline, n-propanol, 2-propanol, formaldehyde, acetaldehyde, hexanal, heptanal, 1-phenylethanone, 2-butanone, and isopropyl myristate/tetradecanoic acid. Changes occurring in the transition from “healthy” to “unhealthy” status can be detected making breath analysis a powerful methodology for lung cancer prevention and many other diseases in general.^[328] In healthy subjects, a concentration between 1–20 ppb is expected while in unhealthy subjects the concentrations raise to 10–100 ppb.^[329] Notably, some literature reports the possibility to distinguish electronically among patients having different diseases, such as lung, breast, colon and prostate cancer via a nanoscale artificial nose.^[330]

To gain further insight in the involved processes, refs. [331,332], investigated the correlation among in vitro VOC production from lung cancer cells and VOC presence in patients’ breath analysis. In ref. [331], among all the studied VOCs, eleven have been detected as markers of lung cancer in patients’ exhaled breath. The results of these studies support the idea that it is possible to distinguish between healthy persons and patients with lung cancer. In ref. [333], however, no reproducible correlation has been typically found between data collected by instrumental analysis and lung cancer but four VOCs of interest for lung cancer diagnosis have been selected: n-hexanal, 1-butanol, 2-butanone, and 2-pentanone with 92% accuracy in patients’ discrimination and 87% in healthy controls. In another recent work,^[334] the concentration of VOC

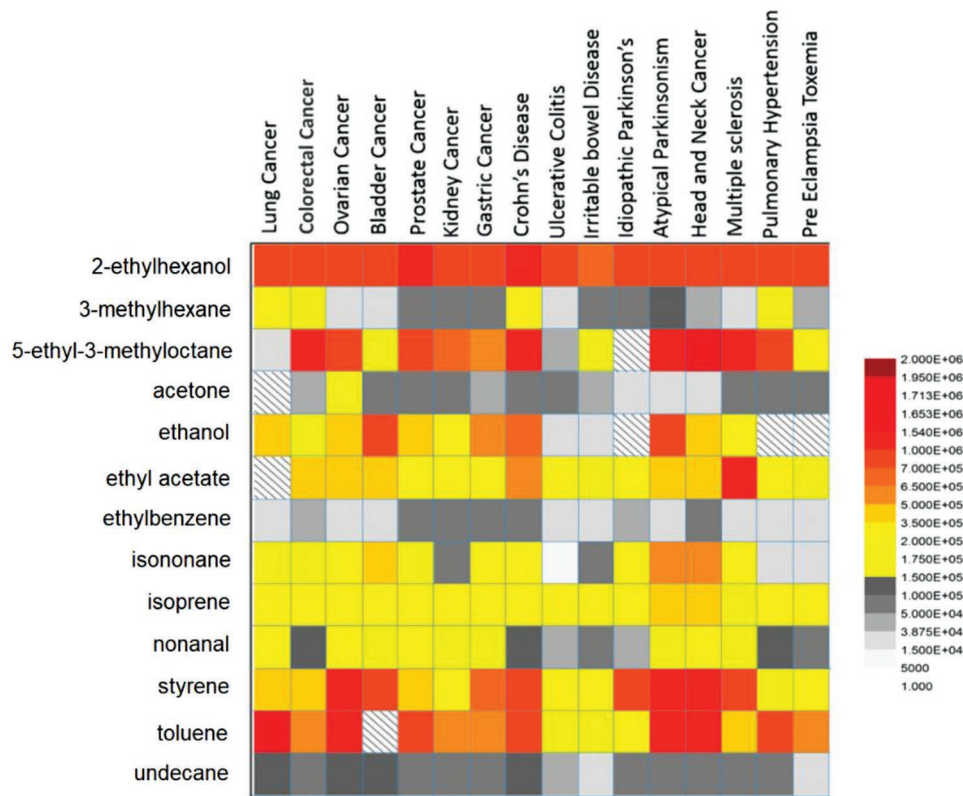


Figure 13. Correlation reported between certain VOCs and human diseases (reproduced with permission.^[341] Copyright 2017, American Chemical Society).

biomarkers in controls and in patients with early-stage lung cancer were shown to be similar and, in addition, the VOCs concentrations are of the order of 0.1 ppb.

The discrepancy of analytical results and conclusions in the relevant literature can be ascribed to a variety of factors. First of all, breath in human being is not standardized: out of 3000+ different VOCs investigated in ref. [329], only 27 were common among all subjects. Most VOCs in the human breath are not generated in the body, but come from food ingestion or exposure to environmental pollutants and thus should be discriminated from pathologies-associated signals.^[329] As a consequence, most breath markers (including VOCs) show ranges of concentrations which vary considerably from one person to another.^[328,335] Some examples of sensors attempting to measure a marker of interest in exhaled breath analysis are ammonia^[336] and acetone and isopropanol^[337] gas sensors specifically optimized for breath analysis. In any case, the field still suffers for lack of standardization in breath sampling and analysis techniques, as evidenced in ref. [335]; in an overview of 10 papers, 170 distinct VOCs were found and only 10 of them appeared at least in two different experiments. Nevertheless, for lung cancer diagnosis, by crossing the information in,^[329,331–335,338] eighteen VOCs of

interest were tentatively extracted: cyclohexane, xylene, ethanol, 2-butanone, isoprene, isopropanol, acetone toluene, decane, nonane, decanal, n-hexanal, n-nonanal, 1-butanol, butane, butanoic acid, and butanal 2-pentanone.

In conclusion, it seems possible that early diagnosis from breath analysis could be achieved in future in reproducible way, but well-defined standardization procedures will be required to discern disease pattern indicators from signals influenced by individuals' lifestyle, gender, diet. In this scenario, it is possible that relevant progresses could be achieved by analyzing time-dependent data and performing differential person-specific measurements.^[339]

In terms of sensing layers, as a matter of fact, initial studies on volatilomics were carried out with analytical techniques such as gas chromatography. Then sensors and e-noses started to be used and macrocycles, polymers, organically capped nanoparticles, metal oxides, and nanocomposites were employed in some of the mentioned references. However, it is expected that nano-materials, nano-heterostructures and composites will define the path to move from some initial lab demonstration to relevant diagnostic technologies due to their ability to provide humidity-resistant gas sensors with LOD in the low ppb range, which is

Table 3. Gas sensing materials with details on their working principle, advantages, and limiting factors.

Active layer material	Working principle	Advantages	Limiting factors
Metal oxides	During a pre-heating phase, oxygen on the surface adsorbs and ionizes and the material becomes sensitive to the gas analytes, for example, leading to variations in electrical resistance	Reliability in response and long-term stability, easiness in miniaturization, high control on the surface chemistry, the reacting species depends on the pre-heating temperature	High temperature operation and high power consumption, poor selectivity, stability toward humidity, less tunable if compared to organic compounds
Mesoporous metal oxides	Measurable response as capacitance variations, resistance variations, optical variations, mass changes	Increased sensitivity due to large surface-to-volume ratios, pore dimensions engineering and use as filter layers for improving selectivity, availability of hierarchical and hollow oxide nanostructures, possible use as host matrices	High working temperature; long recovery time, structure collapsing and/or film cracking due to high working temperatures, resistance drift
Metal oxides nanomaterials and nanoheterostructures	The working principle depends on the material; in general, changes in electrical, weight, optical properties	Increased surface-to-volume ratio, room temperature operation and low power consumption, high sensitivity, good reversibility and selectivity, short response time (ms)	Challenging large-scale production, high fabrication costs
Conductive organic materials (polymers, macrocycles, and molecular aggregates)	Changes in electrical conductivity due to doping–dedoping processes, variations in optical absorption, and polymer weight modifications	Inexpensive fabrication, easy tuning, room-temperature operation and low power consumption, suitability for miniaturization and flexible substrates, short response times and reversible chemical reactions with gases	Generally unstable in the atmosphere and very sensitive to environment-related factors (i.e., moisture), low selectivity
Non-conductive organic compounds (calixarenes, cavitands)	Changes of mass and/or optical properties and/or surface potential	Sensitivity–structure relationship, versatile chemical synthesis, good stability, wide range of chemicals, work at room temperature	Lack of conductivity requires more complex transducers. In general limited sensitivity and selectivity.
Carbon nanotubes, graphene, and 2D materials	Change in electrical properties upon analyte adsorption; functionalization with conductive polymers or metals amplifies sensitivity	Low-noise levels, chemical tunability, wide range of electronic applications	Generally, low selectivity, difficulties in large-scale production, long recovery time, absence of functional groups
Composites	Mainly, changes in electrical properties	Unique combination of properties, application-specific tuning, improved selectivity and sensitivity, reduced operation temperatures	Complex sensing mechanism still not completely understood, tendency to agglomerate in solvents

essential to discern a pathological from a healthy condition. In this case, due to the relevant application, an increased device cost is justified.

Another field of application in the healthcare sector is active ageing and real time monitoring of elderly/sport/vital parameters. The strength of this technology could result in portable and user-friendly diagnostic instruments (i.e., hardware + smartphone app) to make early and continuous physical check available to most of the population.^[340]

4. Conclusions, Challenges, and Perspectives

Due to a widening range of applications and the availability of novel active materials, the gas sensing field is attracting increasing research interest in the last years. Nowadays, novel classes of materials enable relevant performance improvements and application specific tuning. A summary is reported in **Table 3**, including metal oxides, conductive and non-conductive organic materials, mesoporous materials, nanomaterials, 2D materials, nanocomposites and hybrid combinations. The main challenges regard improved selectivity and tunability, high sensitivity and short response time, stability in the long-time and in humid conditions, room-temperature operation, easy device fabrication, and scalability.^[12] The comparison between classes of materials is only qualitative because of the large variability of properties among the different elements of each class. In particular, nano-, 2D, and composite materials showed possibility to overcome some limiting factors associated to traditional active layers based on metal oxides and organic materials (e.g., in terms of selectivity and sensitivity or operating conditions).

As a result, further opportunities for applications emerged, such as in environmental monitoring, food monitoring and breath analysis. Smart gas sensing is a novel area which can be expected to enter in everybody's daily life responding to domestic and industrial demands, also exploiting the Internet of Things paradigm. Miniaturized sensors for real-time environment pollution evaluation are necessary today, according to the new lifestyles and the continuous urbanizations and industrialization of different areas of the world. Future breakthroughs can also lead to early, non-invasive diagnostic tools to face severe pathologies, such as lung cancer, at their early stage.

Avoiding a moisture-dependent response is one of today main challenges for real life applications. Indeed, the device capability to detect a specific gas can be almost totally screened in a humid environment. In general, obtaining a uniform gas sensor specification for all the applications and environments is difficult since gas sensors response is influenced by the atmosphere composition. Advanced signal processing and pattern recognition techniques applied to sensors arrays datasets help to face this issue. The availability of open specification repositories, constantly updated by the Internet of Things, can facilitate this procedure processing the data through a cloud server, for example via artificial neural networks nonlinear classification.^[264]

It is important to remark that due to the large variability of the chemical properties of gases and volatile compounds sensors cannot be based on unique technology or material. Rather, it is necessary a further effort in investigating the sensing

properties of organic and inorganic materials in order to enable the design of efficient sensor systems for selected applications. Such a development is fully justified by the necessity of gas sensors whose market is expected to steadily grow at a rate of 6.25% per year, surpassing 1 billion dollars in 2022.^[264]

Acknowledgements

This work was supported by PON FSE—FESR 2014–2020 (CCI 2014IT16M2OP005)—Axis I “Investments in Human Capital” Action I.1 “Innovative PhDs with industrial characterization”—project DOT1712250 code 3, by the Italian National FISR-CIPE Project “InnoSense”: development of an innovative sensing platform for on-field analysis and monitoring (delibera CIPE n.78 del 07/08/2017), by Italian National PON-AIM1800370-activity 2 (topic Health) and by the Apulia region program “RESEARCH FOR INNOVATION” (REFIN n° 6277F79D-UNISAL036), by PON “Ricerca e Innovazione” 2014-2020, Azione IV.6 “Contratti di ricerca su tematiche Green”.

Open access funding provided by Universita del Salento within the CRUI-CARE Agreement.

Conflict of Interest

The authors declare no conflict of interest.

Keywords

breath analysis, electronic nose, environmental monitoring, food monitoring, gas sensors, signal processing

Received: February 21, 2022

Revised: September 11, 2022

Published online:

- [1] G. Heiland, D. Kohl, *Sens. Actuators* **1985**, *8*, 227.
- [2] J. J. Miasik, A. Hooper, B. C. Tofield, *J. Chem. Soc., Faraday Trans. 1* **1986**, *82*, 117.
- [3] A. G. Abdullayev, A. V. Evdokimov, M. N. Murshudiy, M. I. Scheglov, *Sens. Actuators* **1987**, *11*, 339.
- [4] H. Nanto, H. Sokooshi, T. Kawai, *Sens. Actuators, B* **1993**, *14*, 715.
- [5] N. Funazaki, A. Hemmi, S. Ito, Y. Asano, Y. Yano, N. Miura, N. Yamazoe, *Sens. Actuators, B* **1995**, *25*, 797.
- [6] G. Neri, *Chemosensors* **2015**, *3*, 1.
- [7] A. Mirzaei, S. G. Leonardi, G. Neri, *Ceram. Int.* **2016**, *42*, 15119.
- [8] M. Vanderroost, P. Ragaert, F. Devlieghere, B. De Meulenaer, *Trends Food Sci. Technol.* **2014**, *39*, 47.
- [9] C. Di Natale, R. Paolesse, E. Martinelli, R. Capuano, *Anal. Chim. Acta* **2014**, *824*, 1.
- [10] M. Phillips, V. Basa-Dalay, J. Blais, G. Bothamley, A. Chaturvedi, K. D. Modi, M. Pandya, M. P. R. Natividad, U. Patel, N. N. Ramraje, P. Schmitt, Z. F. Udawadia, *Tuberculosis* **2012**, *92*, 314.
- [11] F. Röck, N. Barsan, U. Weimar, *Chem. Rev.* **2008**, *108*, 705.
- [12] H. Bai, G. Shi, *Sensors* **2007**, *7*, 267.
- [13] V. Kumar, K.-H. Kim, P. Kumar, B.-H. Jeon, J.-C. Kim, *Coord. Chem. Rev.* **2017**, *342*, 80.
- [14] A. Kaushik, R. Kumar, S. K. Arya, M. Nair, B. D. Malhotra, S. Bhansali, *Chem. Rev.* **2015**, *115*, 4571.

- [15] A. Venkatasubramanian, V. T. K. Sauer, S. K. Roy, M. Xia, D. S. Wishart, W. K. Hiebert, *Nano Lett.* **2016**, *16*, 6975.
- [16] D. Kohl, *J. Phys. D: Appl. Phys.* **2001**, *34*, R125.
- [17] J. Hodgkinson, R. P. Tatam, *Meas. Sci. Technol.* **2013**, *24*, 012004.
- [18] T. Seiyama, A. Kato, K. Fujiishi, M. Nagatani, *Anal. Chem.* **1962**, *34*, 1502.
- [19] J. Zhang, X. Liu, G. Neri, N. Pinna, *Adv. Mater.* **2016**, *28*, 795.
- [20] C. Zhang, P. Chen, W. Hu, *Chem. Soc. Rev.* **2015**, *44*, 2087.
- [21] P. Wang, T. Dong, C. Jia, P. Yang, *Sens. Actuators, B* **2019**, *288*, 1.
- [22] K. Wetchakun, T. Samerjai, N. Tamaekong, C. Liewhiran, C. Siriwong, V. Kruefu, A. Wisitsoraat, A. Tuantranont, S. Phanichphant, *Sens. Actuators, B* **2011**, *160*, 580.
- [23] H.-J. Kim, J.-H. Lee, *Sens. Actuators, B* **2014**, *192*, 607.
- [24] T. Wagner, S. Haffer, C. Weinberger, D. Klaus, M. Tiemann, *Chem. Soc. Rev.* **2013**, *42*, 4036.
- [25] E. Rossinyol, A. Prim, E. Pellicer, J. Arbiol, F. Hernández-Ramírez, F. Peiró, A. Cornet, J. R. Morante, L. A. Solovyov, B. Tian, T. Bo, D. Zhao, *Adv. Funct. Mater.* **2007**, *17*, 1801.
- [26] G. S. Devi, T. Hyodo, Y. Shimizu, M. Egashira, *Sens. Actuators, B* **2002**, *87*, 122.
- [27] T. Hyodo, S. Abe, Y. Shimizu, M. Egashira, *Sens. Actuators, B* **2003**, *93*, 590.
- [28] L. G. Teoh, Y. M. Hon, J. Shieh, W. H. Lai, M. H. Hon, *Sens. Actuators, B* **2003**, *96*, 219.
- [29] T. Waitz, T. Wagner, T. Sauerwald, C.-D. Kohl, M. Tiemann, *Adv. Funct. Mater.* **2009**, *19*, 653.
- [30] H.-S. Zhou, T. Yamada, K. Asai, I. Honma, H. Uchida, T. Katsube, *Jpn. J. Appl. Phys., Part 1* **2001**, *40*, 7098.
- [31] B. Sun, J. Horvat, H. S. Kim, W.-S. Kim, J. Ahn, G. Wang, *J. Phys. Chem. C* **2010**, *114*, 18753.
- [32] T. Hyodo, N. Nishida, Y. Shimizu, M. Egashira, *Sens. Actuators, B* **2002**, *83*, 209.
- [33] K. D. Benkstein, S. Semancik, *Sens. Actuators, B* **2006**, *113*, 445.
- [34] T. Yamada, H.-S. Zhou, H. Uchida, M. Tomita, Y. Ueno, T. Ichino, I. Honma, K. Asai, T. Katsube, *Adv. Mater.* **2002**, *14*, 812.
- [35] C. Xu, J. Tamaki, N. Miura, N. Yamazoe, *Sens. Actuators, B* **1991**, *3*, 147.
- [36] J.-H. Lee, *Sens. Actuators, B* **2009**, *140*, 319.
- [37] M. Tiemann, *Chem. Eur. J.* **2007**, *13*, 8376.
- [38] X. Y. Xiao, L. L. Liu, J. H. Ma, Y. Ren, X. W. Cheng, Y. H. Zhu, D. Zhao, A. A. Elzatahry, A. Alghamidi, Y. Deng, *ACS Appl. Mater. Interfaces* **2018**, *10*, 1871.
- [39] Y. Liu, X. Gao, F. Li, G. Lu, T. Zhang, N. Barsan, *Sens. Actuators, B* **2018**, *260*, 927.
- [40] W. Liu, Y. L. Xie, T. X. Chen, Q. X. Lu, S. U. Rehman, L. Zhu, *Sens. Actuators, B* **2019**, *298*, 126871.
- [41] M.-D. Wang, Y.-Y. Li, B.-H. Yao, K. Zhai, Z.-J. Li, H.-C. Yao, *Sens. Actuators, B* **2019**, *288*, 656.
- [42] B. X. Feng, Y. Y. Feng, J. Qin, Z. Wang, Y. L. Zhang, F. Du, Y. Zhao, J. Wei, *Sens. Actuators, B* **2021**, *341*, 129965.
- [43] H. N. Bai, H. Guo, Y. Tan, J. Wang, Y. Dong, B. Liu, Z. Xie, F. Guo, D. Chen, R. Zhang, Y. Zheng, *Sens. Actuators, B* **2021**, *340*, 129924.
- [44] J. H. Ma, Y. Y. Li, J. C. Li, X. Y. Yang, Y. Ren, A. A. Alghamdi, G. Song, K. Yuan, Y. Deng, *Adv. Funct. Mater.* **2021**, *32*, 2107439.
- [45] Y. H. Li, X. R. Zhou, W. Luo, X. W. Cheng, Y. H. Zhu, A. M. El-Toni, A. Khan, Y. Deng, D. Zhao, *Adv. Mater. Interfaces* **2019**, *6*, 1801269.
- [46] W. C. Geng, Z. Y. Ma, J. H. Yang, L. B. Duan, F. Li, Q. Y. Zhang, *Sens. Actuators, B* **2021**, *334*, 129639.
- [47] J. H. Ma, Y. Ren, X. R. Zhou, L. L. Liu, Y. H. Zhu, X. W. Cheng, P. Xu, X. Li, Y. Deng, D. Zhao, *Adv. Funct. Mater.* **2018**, *28*, 1705268.
- [48] P. L. Quang, N. D. Cuong, T. T. Hoa, H. T. Long, C. M. Hung, D. T. T. Le, N. V. Hieu, *Sens. Actuators, B* **2018**, *270*, 158.
- [49] M. P. Chen, H. P. Wang, J. C. Hu, Y. M. Zhang, K. J. Li, D. M. Zhang, S. Zhou, J. Zhang, Z. Zhu, Q. Liu, *Adv. Mater. Interfaces* **2019**, *6*, 1801453.
- [50] G. Dong, H. Fan, H. Tian, J. Fang, Q. Li, *RSC Adv.* **2015**, *5*, 29618.
- [51] M. Drobek, J.-H. Kim, M. Bechelany, C. Vallicari, A. Julbe, S. S. Kim, *ACS Appl. Mater. Interfaces* **2016**, *8*, 8323.
- [52] X. Zhou, X. Cheng, Y. Zhu, A. A. Elzatahry, A. Alghamdi, Y. Deng, D. Zhao, *Chin. Chem. Lett.* **2018**, *29*, 405.
- [53] R. Malik, V. K. Tomer, V. Chaudhary, M. S. Dahiya, S. P. Nehra, S. Duhan, K. Kailasam, *Sens. Actuators, B* **2018**, *255*, 3564.
- [54] S. Rizzato, A. Leo, A. G. Monteduro, M. S. Chiriaco, E. Primiceri, F. Sirsi, A. Milone, G. Maruccio, *Micromachines* **2020**, *11*, 491.
- [55] G. Zhong, G. Bernhardt, R. Lad, S. Collins, R. Smith, in *6th IEEE Sens. Conf.*, IEEE, Atlanta, GA **2007**, pp. 1225–8.
- [56] N. Miura, M. Nakatou, S. Zhuikov, *Sens. Actuators, B* **2003**, *93*, 221.
- [57] Y.-F. Sun, S.-B. Liu, F.-L. Meng, J.-Y. Liu, Z. Jin, L.-T. Kong, J.-H. Liu, *Sensors* **2012**, *12*, 2610.
- [58] K. Suri, S. Annapoorni, A. K. Sarkar, R. P. Tandon, *Sens. Actuators, B* **2002**, *81*, 277.
- [59] M. K. Kennedy, F. E. Kruis, H. Fissan, B. R. Mehta, S. Stappert, G. Dumpich, *J. Appl. Phys.* **2003**, *93*, 551.
- [60] K. H. An, S. Y. Jeong, H. R. Hwang, Y. H. Lee, *Adv. Mater.* **2004**, *16*, 1005.
- [61] W. Y. Li, L. N. Xu, J. Chen, *Adv. Funct. Mater.* **2005**, *15*, 851.
- [62] R. Ionescu, *Sens. Actuators, B* **2005**, *104*, 132.
- [63] J. T. McCue, J. Y. Ying, *Chem. Mater.* **2007**, *19*, 1009.
- [64] D. Barreca, E. Comini, A. P. Ferrucci, A. Gasparotto, C. Maccato, C. Maragno, G. Sberveglieri, E. Tondello, *Chem. Mater.* **2007**, *19*, 5642.
- [65] L. Liao, Z. Zhang, B. Yan, Z. Zheng, Q. L. Bao, T. Wu, C. M. Li, Z. X. Shen, J. X. Zhang, H. Gong, J. C. Li, T. Yu, *Nanotechnology* **2009**, *20*, 085203.
- [66] A. Ponzoni, E. Comini, I. Concina, M. Ferroni, M. Falasconi, E. Gobbi, V. Sberveglieri, G. Sberveglieri, *Sensors* **2012**, *12*, 17023.
- [67] X. Chen, C. K. Y. Wong, C. A. Yuan, G. Zhang, *Sens. Actuators, B* **2013**, *177*, 178.
- [68] K.-R. Park, H.-B. Cho, J. Lee, Y. Song, W.-B. Kim, Y.-H. Choa, *Sens. Actuators, B* **2020**, *302*, 127179.
- [69] X. Fan, Y. Xu, C. Ma, W. He, *J. Alloys Compd.* **2021**, *854*, 157234.
- [70] C. Zhang, L. Li, L. Hou, W. Chen, *Sens. Actuators, B* **2019**, *291*, 130.
- [71] L. Song, L. Yang, Z. Wang, D. Liu, L. Luo, X. Zhu, Y. Xi, Z. Yang, N. Han, F. Wang, Y. Chen, *Sens. Actuators, B* **2019**, *283*, 793.
- [72] G. Namgung, Q. T. H. Ta, W. Yang, J. S. Noh, *ACS Appl. Mater. Interfaces* **2019**, *11*, 1411.
- [73] D. Zhao, H. Huang, S. Chen, Z. Li, S. Li, M. Wang, H. Zhu, X. Chen, *Nano Lett.* **2019**, *19*, 3448.
- [74] D. K. Kwon, Y. Porte, K. Y. Ko, H. Kim, J. M. Myoung, *ACS Appl. Mater. Interfaces* **2018**, *10*, 31505.
- [75] L. Liu, S. Shu, G. Zhang, S. Liu, *ACS Appl. Nano Mater.* **2018**, *1*, 31.
- [76] C. Jiang, G. Zhang, Y. Wu, L. Li, K. Shi, *CrystEngComm* **2012**, *14*, 2739.
- [77] A. Salehi, *Sens. Actuators, B* **2003**, *96*, 88.
- [78] E. Strelcov, S. Dmitriev, B. Button, J. Cothren, V. Sysoev, A. Kolmakov, *Nanotechnology* **2008**, *19*, 355502.
- [79] J.-H. Kim, H. W. Kim, S. S. Kim, *Sens. Actuators, B* **2017**, *251*, 781.
- [80] J. H. Kim, A. Mirzaei, H. W. Kim, S. S. Kim, *ACS Appl. Mater. Interfaces* **2019**, *11*, 24172.
- [81] J. H. Kim, J. Y. Kim, J. H. Lee, A. Mirzaei, H. W. Kim, S. Hishita, S. S. Kim, *Sens. Actuators, B* **2020**, *321*, 128475.
- [82] J. H. Kim, A. Mirzaei, J. Y. Kim, J. H. Lee, H. W. Kim, S. Hishita, S. S. Kim, *Sens. Actuators, B* **2020**, *304*, 127307.
- [83] S. Sayegh, J. H. Lee, D. H. Yang, M. Weber, I. Iatsunskyi, E. Coy, A. Razzouk, S. S. Kim, M. Bechelany, *Sens. Actuators, B* **2021**, *344*, 130302.

- [84] J.-H. Kim, H. Park, A. Mirzaei, M. G. Hahm, S. Ahn, M. Halik, C. Park, S. S. Kim, *Sens. Actuators, B* **2021**, *342*, 130036.
- [85] S. H. Lu, Y. Z. Zhang, J. Y. Liu, H. Y. Li, Z. X. Hu, X. Luo, N. Gao, B. Zhang, J. Jiang, A. Zhong, J. Luo, H. Liu, *Sens. Actuators, B* **2021**, *345*, 130334.
- [86] S. Zeb, X. J. Peng, G. Z. Yuan, X. X. Zhao, C. Y. Qin, G. X. Sun, Y. Nie, Y. Cui, X. Jiang, *Sens. Actuators, B* **2020**, *305*, 127435.
- [87] P. Li, Z. Zhang, Z. Zhuang, J. Guo, Z. Fang, S. L. Fereja, W. Chen, *Anal. Chem.* **2021**, *93*, 7465.
- [88] M. Tonezzer, *Sens. Actuators, B* **2019**, *288*, 53.
- [89] X. Chang, X. Qiao, K. Li, P. Wang, Y. Xiong, X. Li, F. Xia, Q. Xue, *Sens. Actuators, B* **2020**, *317*, 128208.
- [90] D. Gu, X. Wang, W. Liu, X. Li, S. Lin, J. Wang, M. N. Romyantseva, A. M. Gaskov, S. A. Akbar, *Sens. Actuators, B* **2020**, *305*, 127455.
- [91] J. Wang, S. Fan, Y. Xia, C. Yang, S. Komarneni, *J. Hazard. Mater.* **2020**, *381*, 120919.
- [92] N. M. Hung, C. M. Hung, N. V. Duy, N. D. Hoa, H. S. Hong, T. K. Dang, N. N. Viet, L. V. Thong, P. H. Phuoc, N. V. Hieu, *Sens. Actuators, A* **2021**, *327*, 112759.
- [93] Z. P. Tshabalala, T. P. Mokoena, M. Jozela, J. Tshilongo, T. K. Hillie, H. C. Swart, D. E. Motaung, *ACS Appl. Nano Mater.* **2021**, *4*, 702.
- [94] I. S. Jeon, G. Bae, M. Jang, Y. Yoon, S. Jang, W. Song, S. Myung, J. Lim, S. S. Lee, H. Jung, J. Hwang, K. An, *Appl. Surf. Sci.* **2021**, *540*, 148350.
- [95] K.-Q. Peng, X. Wang, S.-T. Lee, *Appl. Phys. Lett.* **2009**, *95*, 243112.
- [96] L. Guan, S. Wang, W. Gu, J. Zhuang, H. Jin, W. Zhang, T. Zhang, J. Wang, *Sens. Actuators, B* **2014**, *196*, 321.
- [97] X. Jiang, S. Qin, Y. Cao, R. Wu, D. Han, Z. Hua, C. Zhu, X. Huang, L. Wang, S. Yang, *ACS Appl. Nano Mater.* **2020**, *3*, 3402.
- [98] Y. Xia, A. F. Pan, D. W. Gardner, S. K. Zhao, A. K. Davey, Z. Li, L. Zhao, C. Carraro, R. Maboudian, *Sens. Actuators, B* **2021**, *344*, 130180.
- [99] S. Nie, D. Dastan, J. Li, W.-D. Zhou, S.-S. Wu, Y.-W. Zhou, X. Yin, *J. Phys. Chem. Solids* **2021**, *150*, 109864.
- [100] Y. Wang, X.-N. Meng, J.-L. Cao, *J. Hazard. Mater.* **2020**, *381*, 120944.
- [101] W.-D. Zhou, D. Dastan, J. Li, X.-T. Yin, Q. Wang, *Nanomaterials* **2020**, *10*, 785.
- [102] Z. M. Yang, D. Z. Zhang, D. Y. Wang, *Sens. Actuators, B* **2020**, *304*, 127369.
- [103] A. V. Raghu, K. K. Karuppanan, B. Pullithadathil, *ACS Sens.* **2018**, *3*, 1811.
- [104] C.-L. Hsu, B.-Y. Jhang, C. Kao, T.-J. Hsueh, *Sens. Actuators, B* **2018**, *274*, 565.
- [105] K. Lee, D.-H. Baek, H. Na, J. Choi, J. Kim, *Sens. Actuators, B* **2018**, *265*, 522.
- [106] V. T. Duoc, C. M. Hung, H. Nguyen, N. V. Duy, N. V. Hieu, N. D. Hoa, *Sens. Actuators, B* **2021**, *348*, 130652.
- [107] J. H. Kim, A. Mirzaei, H. W. Kim, S. S. Kim, *Sens. Actuators, B* **2020**, *302*, 127150.
- [108] X. Yang, H. Fu, L. Zhang, X. An, S. Xiong, X. Jiang, A. Yu, *Sens. Actuators, B* **2019**, *286*, 483.
- [109] Z. Cai, S. Park, *Sens. Actuators, B* **2020**, *322*, 128651.
- [110] J.-H. Kim, A. Mirzaei, H. W. Kim, S. S. Kim, *Sens. Actuators, B* **2018**, *267*, 597.
- [111] J. H. Lee, A. Mirzaei, J. Y. Kim, J. H. Kim, H. W. Kim, S. S. Kim, *Sens. Actuators, B* **2020**, *302*, 127194.
- [112] J.-H. Kim, J.-H. Lee, Y. Park, J.-Y. Kim, A. Mirzaei, H. W. Kim, S. S. Kim, *Sens. Actuators, B* **2019**, *294*, 78.
- [113] M. Tonezzer, J.-H. Kim, J.-H. Lee, S. Iannotta, S. S. Kim, *Sens. Actuators, B* **2019**, *281*, 670.
- [114] P.-L. Chen, I.-P. Liu, W.-C. Chen, J.-S. Niu, W.-C. Liu, *Sens. Actuators, B* **2020**, *322*, 128592.
- [115] T. F. Weng, M. S. Ho, C. Sivakumar, B. Balraj, P. F. Chung, *Appl. Surf. Sci.* **2020**, *533*, 147476.
- [116] H. Zhang, Y. Wang, X. Zhu, Y. Li, W. Cai, *Sens. Actuators, B* **2019**, *280*, 192.
- [117] S. Rizzato, E. Primiceri, A. G. Monteduro, A. Colombelli, A. Leo, M. G. Manera, R. Rella, G. Maruccio, *Beilstein J. Nanotechnol.* **2018**, *9*, 1582.
- [118] Y. Wang, C. Liu, Z. Wang, Z. Song, X. Zhou, N. Han, Y. Chen, *Sens. Actuators, B* **2019**, *278*, 28.
- [119] H.-J. Cho, V. T. Chen, S. Qiao, W.-T. Koo, R. M. Penner, I.-D. Kim, *ACS Sens.* **2018**, *3*, 2152.
- [120] E. Navarrete, C. Bittencourt, X. Noirfalise, P. Urnek, E. Gonzalez, F. Guell, E. Llobet, *Sens. Actuators, B* **2019**, *298*, 126868.
- [121] T. T. N. Hoa, N. V. Duy, C. M. Hung, N. V. Hieu, H. H. Hau, N. D. Hoa, *RSC Adv.* **2020**, *10*, 17713.
- [122] K. P. Yuan, C. Y. Wang, L. Y. Zhu, Q. Cao, J. H. Yang, X. X. Li, W. Huang, Y. Wang, H. Lu, D. W. Zhang, *ACS Appl. Mater. Interfaces* **2020**, *12*, 14095.
- [123] R. Zhang, S. Cao, T. T. Zhou, T. Fei, R. Wang, T. Zhang, *Sens. Actuators, B* **2020**, *310*, 127695.
- [124] B. Bouchikhi, T. Chludzinski, T. Saidi, J. Smulko, N. El Bari, H. Wen, R. Ionescu, *Sens. Actuators, B* **2020**, *320*, 128331.
- [125] R. Xing, L. Xu, J. Song, C. Zhou, Q. Li, D. Liu, H. W. Song, *Sci. Rep.* **2015**, *5*, 14.
- [126] W. Wang, X. Liu, S. Mei, Y. Jia, M. Liu, X. Xue, D. Yang, *Sens. Actuators, B* **2019**, *287*, 157.
- [127] I. Fratoddi, I. Venditti, C. Cametti, M. V. Russo, *Sens. Actuators, B* **2015**, *220*, 534.
- [128] C. O. Baker, X. Huang, W. Nelson, R. B. Kaner, *Chem. Soc. Rev.* **2017**, *46*, 1510.
- [129] L. Xue, W. Wang, Y. Guo, G. Liu, P. Wan, *Sens. Actuators, B* **2017**, *244*, 47.
- [130] N. R. Tanguy, M. Thompson, N. Yan, *Sens. Actuators, B* **2018**, *257*, 1044.
- [131] N. Mkhize, K. Murugappan, M. R. Castell, H. Bhaskaran, *J. Mater. Chem. C* **2021**, *9*, 4591.
- [132] C. Yu, J. H. He, X. F. Cheng, H. Z. Lin, H. Yu, J. M. Lu, *Angew. Chem., Int. Ed.* **2021**, *60*, 15328.
- [133] T. Shaymurat, Q. Tang, Y. Tong, L. Dong, Y. Liu, *Adv. Mater.* **2013**, *25*, 2269.
- [134] M. Jang, S. K. Kim, J. Lee, S. Ji, W. Song, S. Myung, J. Lim, S. S. Lee, H.-K. Jung, J. Lee, K.-S. An, *J. Mater. Chem. C* **2019**, *7*, 14504.
- [135] D. H. Kwak, Y. Seo, J. E. Anthony, S. Kim, J. Hur, H. Chae, H. J. Park, B. Kim, E. Lee, S. Ko, W. H. Lee, *Adv. Mater. Interfaces* **2020**, *7*, 1901696.
- [136] X. Zhou, Z. Wang, R. Song, Y. Zhang, L. Zhu, D. Xue, L. Huang, L. Chi, *J. Mater. Chem. C* **2021**, *9*, 1584.
- [137] E. S. Shin, J. Y. Go, G. S. Ryu, A. Liu, Y. Y. Noh, *ACS Appl. Mater. Interfaces* **2021**, *13*, 4278.
- [138] J. H. Lee, Y. Seo, Y. D. Park, J. E. Anthony, D. H. Kwak, J. A. Lim, S. Ko, H. W. Jang, K. Cho, W. H. Lee, *Sci. Rep.* **2019**, *9*, 21.
- [139] L. Torsi, A. Dodabalapur, L. Sabbatini, P. G. Zamboni, *Sens. Actuators, B* **2000**, *67*, 312.
- [140] M. Bouvet, *Anal. Bioanal. Chem.* **2006**, *384*, 366.
- [141] Z. Wang, L. Huang, X. Zhu, X. Zhou, L. Chi, *Adv. Mater.* **2017**, *29*, 1703192.
- [142] D. S. Anisimov, V. P. Chekusova, A. A. Trul, A. A. Abramov, O. V. Borshchev, E. V. Agina, S. A. Ponomarenko, *Sci. Rep.* **2021**, *11*, 10683.
- [143] J. Robertson, *Rep. Prog. Phys.* **2006**, *69*, 327.
- [144] H. Im, X.-J. Huang, B. Gu, Y.-K. Choi, *Nat. Nanotechnol.* **2007**, *2*, 430.
- [145] E. Rahman, A. Shadman, I. Ahmed, S. U. Z. Khan, Q. D. M. Khosru, *Nanotechnology* **2018**, *29*, 235203.

- [146] A. G. Monteduro, Z. Ameer, M. Martino, A. P. Caricato, V. Tasco, I. C. Lekshmi, R. Rinaldi, A. Hazarika, D. Choudhury, D. D. Sarma, G. Maruccio, *J. Mater. Chem. C* **2016**, *4*, 1080.
- [147] A. G. Monteduro, Z. Ameer, S. Rizzato, M. Martino, A. P. Caricato, V. Tasco, I. C. Lekshmi, A. Hazarika, D. Choudhury, D. D. Sarma, G. Maruccio, *J. Phys. D: Appl. Phys.* **2016**, *49*, 405303.
- [148] L. Pirondini, E. Dalcanale, *Chem. Soc. Rev.* **2007**, *36*, 695.
- [149] R. Q. Lu, S. X. L. Luo, Q. He, A. Concellón, T. M. Swager, *Adv. Funct. Mater.* **2021**, *31*, 2007281.
- [150] S. Fanget, S. Hentz, P. Puget, J. Arcamone, M. Matheron, E. Colinet, P. Andreucci, L. Duraffourg, Ed. Myers, M. L. Roukes, *Sens. Actuators, B* **2011**, *160*, 804.
- [151] K. Länge, B. E. Rapp, M. Rapp, *Anal. Bioanal. Chem.* **2008**, *391*, 1509.
- [152] B. Liu, X. Chen, H. Cai, M. M. Ali, X. Tian, L. Tao, Y. Yang, T. Ren, *J. Semicond.* **2016**, *37*, 021001.
- [153] P. Delsing, A. N. Cleland, M. J. A. Schuetz, J. Knörzer, G. Giedke, J. I. Cirac, K. Srinivasan, M. Wu, K. C. Balram, C. Béuerle, T. Meunier, C. J. B. Ford, P. V. Santos, E. Cerda-Méndez, H. Wang, H. J. Krenner, E. D. S. Nysten, M. Weiß, G. R. Nash, L. Thevenard, C. Gourdon, P. Rovillain, M. Marangolo, J.-Y. Duquesne, G. Fischerauer, W. Ruile, A. Reiner, B. Paschke, D. Denysenko, D. Volkmer, et al, *J. Phys. D: Appl. Phys.* **2019**, *52*, 353001.
- [154] S. Rizzato, M. Scigliuzzo, M. S. Chiriaco, P. Scarlino, A. G. Monteduro, C. Maruccio, V. Tasco, G. Maruccio, *J. Micro-mech. Microeng.* **2017**, *27*, 125002.
- [155] M. S. Chiriaco, S. Rizzato, E. Primiceri, S. Spagnolo, A. G. Monteduro, F. Ferrara, G. Maruccio, *Microelectron. Eng.* **2018**, *202*, 31.
- [156] A. Venema, E. Nieuwkoop, M. J. Vellekoop, M. S. Nieuwenhuizen, A. W. Barendsz, *Sens. Actuators* **1986**, *10*, 47.
- [157] M. S. Nieuwenhuizen, A. J. Nederlof, *Sens. Actuators, B* **1990**, *2*, 97.
- [158] A. Mauder, *Sens. Actuators, B* **1995**, *26*, 187.
- [159] Y. J. Lee, H. B. Kim, Y. R. Roh, H. M. Cho, S. Baik, *Sens. Actuators, A* **1998**, *64*, 173.
- [160] N. Ledermann, P. Murali, J. Baborowski, M. Forster, J.-P. Pellaux, *J. Micromech. Microeng.* **2004**, *14*, 1650.
- [161] M. Rapp, J. Reibel, A. Voigt, M. Balzer, O. Bülow, *Sens. Actuators, B* **2000**, *65*, 169.
- [162] X. Chen, M. Cao, Y. Li, W. Hu, P. Wang, K. Ying, H. Pan, *Meas. Sci. Technol.* **2005**, *16*, 1535.
- [163] I. A. Koshets, Z. I. Kazantseva, Y. M. Shirshov, S. A. Cherenok, V. I. Kalchenko, *Sens. Actuators, B* **2005**, *106*, 177.
- [164] J. Devkota, P. Ohodnicki, D. Greve, *Sensors* **2017**, *17*, 801.
- [165] A. Oprea, U. Weimar, *Anal. Bioanal. Chem.* **2019**, *411*, 1761.
- [166] R. Pinalli, A. Pedrini, E. Dalcanale, *Chemistry* **2018**, *24*, 1010.
- [167] C. K. McGinn, Z. A. Lampert, I. Kyriassis, *ACS Sens.* **2020**, *5*, 1514.
- [168] S. Kumar, S. Chawla, M. C. Zou, *J. Inclusion Phenom. Macrocyclic Chem.* **2017**, *88*, 129.
- [169] C. Di Natale, C. P. Gros, R. Paolesse, *Chem. Soc. Rev.* **2022**, *51*, 1277.
- [170] Z. Jin, Y. Su, Y. Duan, *Sens. Actuators, B* **2001**, *72*, 75.
- [171] Z. Z. Zhou, Y. Z. Xu, C. D. Qiao, L. B. Liu, Y. X. Jia, *Sens. Actuators, B* **2021**, *332*, 129482.
- [172] P. Colson, C. Henrist, R. Cloots, *J. Nanomater.* **2013**, *2013*, 948510.
- [173] Y. Yan, G. Yang, J.-L. Xu, M. Zhang, C.-C. Kuo, S.-D. Wang, *Sci. Technol. Adv. Mater.* **2021**, *21*, 768.
- [174] J. J. Belbruno, *Chem. Rev.* **2019**, *119*, 94.
- [175] O. I. Parisi, F. Francornano, M. Dattilo, F. Patitucci, S. Prete, F. Amone, F. Puoci, *J. Funct. Biomater.* **2022**, *13*, 12.
- [176] M. Zarejousheghani, P. Rahimi, H. Borsdorf, S. Zimmermann, Y. Joseph, *Sensors* **2021**, *21*, 2406.
- [177] Y. Zhang, J. Zhang, Q. Liu, *Sensors* **2017**, *17*, 1567.
- [178] X. Tang, J.-P. Raskin, D. Lahem, A. Krumpmann, A. Decroly, M. Debliquy, *Sensors* **2017**, *17*, 675.
- [179] E. Aznar-Gadea, I. Sanchez-Alarcon, A. Soosaimanickam, P. J. Rodriguez-Canto, F. Perez-Pla, J. P. Martínez-Pastor, R. Abargues, *J. Mater. Chem. C* **2022**, *10*, 1754.
- [180] R. Liang, L. Chen, W. Qin, *Sci. Rep.* **2015**, *5*, 9.
- [181] Y. B. Wei, Q. Zeng, J. Z. Huang, X. R. Guo, L. L. Wang, L. S. Wang, *ACS Appl. Mater. Interfaces* **2020**, *12*, 24363.
- [182] M. C. Lonergan, E. J. Severin, B. J. Doleman, S. A. Beaber, R. H. Grubbs, N. S. Lewis, *Chem. Mater.* **1996**, *8*, 2298.
- [183] E. Llobet, *Sens. Actuators, B* **2013**, *179*, 32.
- [184] V. Schroeder, S. Savagatrup, M. He, S. Lin, T. M. Swager, *Chem. Rev.* **2019**, *119*, 599.
- [185] M. N. Norizan, M. H. Moklis, S. Z. N. Demon, N. A. Halim, A. Samsuri, I. S. Mohamad, V. F. Knight, N. Abdullah, *RSC Adv.* **2020**, *10*, 43704.
- [186] T. Han, A. Nag, S. C. Mukhopadhyay, Y. Xu, *Sens. Actuators, A* **2019**, *291*, 107.
- [187] M. Penza, M. Alvisi, R. Rossi, E. Serra, R. Paolesse, A. D'Amico, C. Di Natale, *Nanotechnology* **2011**, *22*, 125502.
- [188] A. T. C. Johnson, S. M. Khamis, G. Preti, J. Kwak, A. Gelperin, *IEEE Sens. J.* **2010**, *10*, 159.
- [189] R. Paolesse, S. Nardis, D. Monti, M. Stefanelli, C. Di Natale, *Chem. Rev.* **2017**, *117*, 2517.
- [190] P. Clément, S. Korom, C. Struzzi, E. J. Parra, C. Bittencourt, P. Ballester, E. Llobet, *Adv. Funct. Mater.* **2015**, *25*, 4011.
- [191] J. H. Bang, A. Mirzaei, M. S. Choi, S. Han, H. Y. Lee, S. S. Kim, H. W. Kim, *Sens. Actuators, B* **2021**, *344*, 130176.
- [192] M. Inaba, T. Oda, M. Kono, N. Phansiri, T. Morita, S. Nakahara, M. Nakano, J. Suehiro, *Sens. Actuators, B* **2021**, *344*, 130257.
- [193] N. D. Chinh, N. M. Hung, S. Majumder, C. Kim, D. Kim, *Sens. Actuators, B* **2021**, *326*, 128956.
- [194] A. K. Geim, K. S. Novoselov, *Nat. Mater.* **2007**, *6*, 183.
- [195] S. Basu, P. Bhattacharyya, *Sens. Actuators, B* **2012**, *173*, 1.
- [196] S. Rizzato, A. G. Monteduro, A. Leo, M. T. Todaro, G. Maruccio, *Electrochem. Sci. Adv.* **2022**, e2200006.
- [197] F. Schedin, A. K. Geim, S. V. Morozov, E. W. Hill, P. Blake, M. I. Katsnelson, K. S. Novoselov, *Nat. Mater.* **2007**, *6*, 652.
- [198] R. Pearce, T. Iakimov, M. Andersson, L. Hultman, A. L. Spetz, R. Yakimova, *Sens. Actuators, B* **2011**, *155*, 451.
- [199] N. Hu, Y. Wang, J. Chai, R. Gao, Z. Yang, E. S.-W. Kong, Y. Zhang, *Sens. Actuators, B* **2012**, *163*, 107.
- [200] G. H. Lu, L. E. Ocola, J. H. Chen, *Nanotechnology* **2009**, *20*, 445502.
- [201] G. Lu, S. Park, K. Yu, R. S. Ruoff, L. E. Ocola, D. Rosenmann, J. Chen, *ACS Nano* **2011**, *5*, 1154.
- [202] S. Rummyantsev, G. Liu, M. S. Shur, R. A. Potyailo, A. A. Balandin, *Nano Lett.* **2012**, *12*, 2294.
- [203] G. Lu, L. E. Ocola, J. Chen, *Nanotechnology* **2009**, *20*, 445502.
- [204] M. Kooti, S. Keshtkar, M. Askarieh, A. Rashidi, *Sens. Actuators, B* **2019**, *281*, 96.
- [205] L. Z. Zhang, J. N. Shi, Y. H. Huang, H. Y. Xu, K. W. Xu, P. K. Chu, F. Ma, *ACS Appl. Mater. Interfaces* **2019**, *11*, 12958.
- [206] C. Zhao, H. Gong, H. Lan, R. Ramachandran, H. Xu, S. Liu, F. Wang, *Sens. Actuators, B* **2018**, *258*, 492.
- [207] J. Zhang, H. Lu, C. Yan, Z. Yang, G. Zhu, J. Gao, F. Yin, C. Wang, *Sens. Actuators, B* **2018**, *264*, 128.
- [208] X. An, J. C. Yu, Y. Wang, Y. Hu, X. Yu, G. Zhang, *J. Mater. Chem.* **2012**, *22*, 8525.
- [209] Y. Seekaew, A. Wisitsoraat, D. Phokharatkul, C. Wongchoosuk, *Sens. Actuators, B* **2019**, *279*, 69.
- [210] G. Murali, M. Reddeppa, C. S. Reddy, S. Park, T. Chandrakalavathi, M. D. Kim, I. In, *ACS Appl. Mater. Interfaces* **2020**, *12*, 13428.

- [211] Z. Zhang, X. Zou, L. Xu, L. Liao, W. Liu, J. Ho, X. Xiao, C. Jiang, J. Li, *Nanoscale* **2015**, *7*, 10078.
- [212] R. X. Mo, D. Q. Han, C. W. Yang, J. Y. Tang, F. Wang, C. L. Li, *Sens. Actuators, B* **2021**, *330*, 129326.
- [213] C. Zou, J. Hu, Y. J. Su, Z. H. Zhou, B. F. Cai, Z. J. Tao, T. Huo, N. Hu, Y. Zhang, *Sens. Actuators, B* **2020**, *306*, 127546.
- [214] B. Zhang, G. Liu, M. Cheng, Y. Gao, L. Zhao, S. Li, F. Liu, X. Yan, T. Zhang, P. Sun, G. Lu, *Sens. Actuators, B* **2018**, *261*, 252.
- [215] L. S. K. Achary, A. Kumar, B. Barik, P. S. Nayak, N. Tripathy, J. P. Kar, P. Dash, *Sens. Actuators, B* **2018**, *272*, 100.
- [216] L. Guo, X. Kou, M. Ding, C. Wang, L. Dong, H. Zhang, C. Feng, Y. Sun, Y. Gao, P. Sun, G. Lu, *Sens. Actuators, B* **2017**, *244*, 233.
- [217] M. Reddeppa, T. Chandrakalavathi, B. G. Park, G. Murali, R. Siranjeevi, G. Nagaraju, J. S. Yu, R. Jayalakshmi, S. Kim, M. Kim, *Sens. Actuators, B* **2020**, *307*, 127649.
- [218] A. Bag, D. B. Moon, K. H. Park, C. Y. Cho, N. E. Lee, *Sens. Actuators, B* **2019**, *296*, 126684.
- [219] D. Pawar, R. Kanawade, A. Kumar, C. N. Rao, P. J. Cao, S. Gaware, D. Late, S. N. Kale, S. T. Navale, W. J. Liu, D. L. Zhu, Y. M. Lu, R. K. Sinha, *Sens. Actuators, B* **2020**, *312*, 127921.
- [220] Y. Guo, T. Wang, F. Chen, X. Sun, X. Li, Z. Yu, P. Wan, X. Chen, *Nanoscale* **2016**, *8*, 12073.
- [221] Y. Kim, S. Lee, J. G. Song, K. Y. Ko, W. J. Woo, S. W. Lee, M. Park, H. Lee, Z. Lee, H. Choi, W. Kim, J. Park, H. Kim, *Adv. Funct. Mater.* **2020**, *30*, 2003360.
- [222] M. Ikram, Y. Liu, H. Lv, L. Liu, A. U. Rehman, K. Kan, W. Zhang, L. He, Y. Wang, R. Wang, K. Shi, *Appl. Surf. Sci.* **2019**, *466*, 1.
- [223] E. Lee, Y. S. Yoon, D.-J. Kim, *ACS Sens.* **2018**, *3*, 2045.
- [224] R. Kumar, N. Goel, M. Hojamberdiev, M. Kumar, *Sens. Actuators, A* **2020**, *303*, 111875.
- [225] W. Li, R. Chen, W. Qi, L. Cai, Y. Sun, M. Sun, C. Li, X. Yang, L. Xiang, D. Xie, T. Ren, *ACS Sens.* **2019**, *4*, 2809.
- [226] H. J. Park, W.-J. Kim, H.-K. Lee, D.-S. Lee, J.-H. Shin, Y. Jun, Y. J. Yun, *Sens. Actuators, B* **2018**, *257*, 846.
- [227] D. Zhang, J. Liu, C. Jiang, A. Liu, B. Xia, *Sens. Actuators, B* **2017**, *240*, 55.
- [228] B. Sharma, A. Sharma, J. H. Myung, *Sens. Actuators, B* **2021**, *331*, 129464.
- [229] L. Kou, T. Frauenheim, C. Chen, *J. Phys. Chem. Lett.* **2014**, *5*, 2675.
- [230] T. Kaewmaraya, L. Ngamwongwan, P. Moontragoon, W. Jarernboon, D. Singh, R. Ahuja, A. Karton, T. Hussain, *J. Hazard. Mater.* **2021**, *401*, 123340.
- [231] J. Prasongkit, V. Shukla, A. Grigoriev, R. Ahuja, V. Amornkitbamrung, *Appl. Surf. Sci.* **2019**, *497*, 143660.
- [232] W. Choi, N. Choudhary, G. H. Han, J. Park, D. Akinwande, Y. H. Lee, *Mater. Today* **2017**, *20*, 116.
- [233] M. Donarelli, S. Prezioso, F. Perrozzi, F. Bisti, M. Nardone, L. Giancaterini, C. Cantalini, L. Ottaviano, *Sens. Actuators, B* **2015**, *207*, 602.
- [234] W.-N. Zhao, N. Yun, Z.-H. Dai, Y.-F. Li, *RSC Adv.* **2020**, *10*, 1261.
- [235] S. Wang, B. Liu, Z. Duan, Q. Zhao, Y. Zhang, G. Xie, Y. Jiang, S. Li, H. Tai, *Sens. Actuators, B* **2021**, *327*, 128923.
- [236] J. Choi, Y. J. Kim, S. Y. Cho, K. Park, H. Kang, S. J. Kim, H. T. Jung, *Adv. Funct. Mater.* **2020**, *30*, 2003998.
- [237] S. H. Lee, W. Eom, H. Shin, R. B. Ambade, J. H. Bang, H. W. Kim, T. H. Han, *ACS Appl. Mater. Interfaces* **2020**, *12*, 10434.
- [238] Y. Geng, Y. Ren, X. Wang, J. Li, L. Portilla, Y. Fang, J. Zhao, *Sens. Actuators, B* **2022**, *360*, 131633.
- [239] Z. J. Kang, D. Z. Zhang, T. T. Li, X. H. Liu, X. S. Song, *Sens. Actuators, B* **2021**, *345*, 130299.
- [240] Q. Hu, Z. M. Wang, J. Y. Chang, P. Wan, J. H. Huang, L. Feng, *Sens. Actuators, B* **2021**, *344*, 130179.
- [241] D. M. Han, X. H. Li, F. M. Zhang, F. B. Gu, Z. H. Wang, *Sens. Actuators, B* **2021**, *340*, 129990.
- [242] M. Sinha, S. Neogi, R. Mahapatra, S. Krishnamurthy, R. Ghosh, *Sens. Actuators, B* **2021**, *336*, 129729.
- [243] A. G. El-Shamy, *Sens. Actuators, B* **2021**, *329*, 129154.
- [244] L. F. He, C. P. Gao, L. Yang, K. Zhang, X. F. Chu, S. M. Liang, D. Zeng, *Sens. Actuators, B* **2020**, *306*, 127453.
- [245] W. Li, D. Kim, *J. Mater. Sci.* **2010**, *46*, 1857.
- [246] W. Li, N. D. Hoa, Y. Cho, D. Kim, J.-S. Kim, *Sens. Actuators, B* **2009**, *143*, 132.
- [247] S. Gai, B. Wang, X. Wang, R. Zhang, S. Miao, Y. Wu, *Sens. Actuators, B* **2022**, *357*, 131352.
- [248] S.-W. Chiu, K.-T. Tang, *Sensors* **2013**, *13*, 14214.
- [249] B. Malnic, J. Hirono, T. Sato, L. B. Buck, *Cell* **1999**, *96*, 713.
- [250] C. Bushdid, M. O. Magnasco, L. B. Vosshall, A. Keller, *Science* **2014**, *343*, 1370.
- [251] K. Persaud, G. Dodd, *Nature* **1982**, *299*, 352.
- [252] A. Mashukova, M. Spehr, H. Hatt, E. M. Neuhaus, *J. Neurosci.* **2006**, *26*, 9902.
- [253] A. Wilson, M. Baietto, *Sensors* **2009**, *9*, 5099.
- [254] J. W. Gardner, P. N. Bartlett, *Sens. Actuators, B* **1994**, *18*, 210.
- [255] A. Loutfi, S. Coradeschi, G. K. Mani, P. Shankar, J. B. B. Rayappan, *J. Food Eng.* **2015**, *144*, 103.
- [256] M. B. Banerjee, R. B. Roy, B. Tudu, R. Bandyopadhyay, N. Bhattacharyya, *J. Food Eng.* **2019**, *244*, 55.
- [257] I. T. Jolliffe, *Principal Component Analysis*, 2nd ed., Springer, New York **2002**
- [258] V. B. Raj, H. Singh, A. T. Nimal, M. U. Sharma, V. Gupta, *Sens. Actuators, B* **2013**, *178*, 636.
- [259] S. Srivastava, S. Sadisatp, *J. Food Meas. Charact.* **2015**, *10*, 1.
- [260] H.-P. Hsu, J.-S. Shih, *J. Chin. Chem. Soc.* **2006**, *53*, 815.
- [261] J. Zhang, Y. Xue, Q. Sun, T. Zhang, Y. Chen, W. Yu, Y. Xiuong, X. Wei, G. Yu, H. Wan, P. Wang, *Sens. Actuators, B* **2021**, *326*, 128822.
- [262] A. A. S. Ali, A. Farhat, S. Mohamad, A. Amira, F. Bensaali, M. Benammar, A. Bermak, *IEEE Sens. J.* **2018**, *18*, 4633.
- [263] P. Ekins, J. Gupta, P. Boileau, Global Environment Outlook–GEO-6: healthy planet, healthy people, **2019**.
- [264] S. Feng, F. Farha, Q. Li, Y. Wan, Y. Xu, T. Zhang, H. Ning, *Sensors* **2019**, *19*, 3760.
- [265] A. Ghosh, C. Zhang, S. Q. Shi, H. Zhang, *Clean: Soil, Air, Water* **2019**, *47*, 1800491.
- [266] National Center for Biotechnology Information, PubChem Compound Summary for CID 313, Hydrochloric acid., **2004**.
- [267] S. C. K. Misra, P. Mathur, M. Yadav, M. K. Tiwari, S. C. Garg, P. Tripathi, *Polymer* **2004**, *45*, 8623.
- [268] R. J. Cooling, *The British Journal of Ophthalmology* **1987**, *71*, 723.
- [269] J. Gong, Y. Li, Z. Hu, Z. Zhou, Y. Deng, *J. Phys. Chem. C* **2010**, *114*, 9970.
- [270] J.-H. Lim, N. Phiboolsirichit, S. Mubeen, M. A. Deshusses, A. Mulchandani, N. V. Myung, *Nanotechnology* **2010**, *21*, 075502.
- [271] N. Sayed, *Indian Journal of Medical Research* **2006**, *123*, 96.
- [272] World Health Organization, Evolution of WHO air quality guidelines: past, present and future. Copenhagen: WHO Regional Office for Europe **2017**, 39.
- [273] M. D. Shirsat, M. A. Bangar, M. A. Deshusses, N. V. Myung, A. Mulchandani, *Appl. Phys. Lett.* **2009**, *94*, 083502.
- [274] L. Zhou, F. Shen, X. Tian, D. Wang, T. Zhang, W. Chen, *Nanoscale* **2013**, *5*, 1564.
- [275] World Health Organization, WHO guidelines for indoor air quality: selected pollutants: World Health Organization. Regional Office for Europe, **2010**.

- [276] Z. Hoheráková, F. Opekar, *Sens. Actuators, B* **2004**, *97*, 379.
- [277] World Health Organization, Nitrogen Oxides -Environmental Health Criteria 1997, 188.
- [278] S. C. K. Misra, P. Mathur, B. K. Srivastava, *Sens. Actuators, A* **2004**, *114*, 30.
- [279] R. Kurokawa, S. I. Hirano, Y. Ichikawa, G. Matsuo, Y. Takefuji, *Medical gas research* **2019**, *9*, 160.
- [280] A. Simo, B. Mwakikunga, B. T. Sone, B. Julies, R. Madjoe, M. Maaza, *Int. J. Hydrogen Energy* **2014**, *39*, 8147.
- [281] World Health Organization, Air quality guidelines: global update 2005: particulate matter, ozone, nitrogen dioxide, and sulfur dioxide: World Health Organization, **2006**.
- [282] S. Das, S. Chakraborty, O. Parkash, D. Kumar, S. Bandyopadhyay, S. K. Samudrala, A. Sen, H. S. Maiti, *Talanta* **2008**, *75*, 385.
- [283] D. L. García-González, R. Aparicio, *Food Chem.* **2010**, *120*, 572.
- [284] E. Núñez-Carmona, M. Abbatangelo, V. Sberveglieri, *Sensors* **2021**, *21*, 4266.
- [285] M. Alizadeh-Sani, M. Tavassoli, E. Mohammadian, A. Ehsani, G. J. Khaniki, R. Priyadarshi, J.-W. Rhim, *Int. J. Biol. Macromol.* **2021**, *166*, 741.
- [286] Z. Ma, P. Chen, W. Cheng, K. Yan, L. Pan, Y. Shi, G. Yu, *Nano Lett.* **2018**, *18*, 4570.
- [287] M. Senapati, P. P. Sahu, *Biosens. Bioelectron.* **2020**, *168*, 112570.
- [288] W.-Y. Chung, G. T. Le, T. V. Tran, N. H. Nguyen, *Sens. Actuators, B* **2017**, *248*, 910.
- [289] A. M. Bratu, M. Petrus, C. Popa, *Materials* **2020**, *13*, 2694.
- [290] A. Beniwal, Sunny, *J. Food Meas. Charact.* **2018**, *13*, 857.
- [291] N. M. Shaalan, F. Ahmed, S. Kumar, A. Melaibari, P. M. Z. Hasan, A. Aljaafari, *ACS Omega* **2020**, *5*, 30531.
- [292] Z. Kovacs, Z. Bodor, J.-L. Z. Zaukuu, T. Kaszab, G. Bazar, T. Tóth, C. Mohácsi-Farkas, *Foods* **2020**, *9*, 1539.
- [293] S. Capone, M. Epifani, F. Quaranta, P. Siciliano, A. Taurino, L. Vasanelli, *Sens. Actuators, B* **2001**, *78*, 174.
- [294] N. Magan, A. Pavlou, I. Chrysanthakis, *Sens. Actuators, B* **2001**, *72*, 28.
- [295] B. Wang, S. Xu, D.-W. Sun, *Food Res. Int.* **2010**, *43*, 255.
- [296] Å. Eriksson, K. P. Waller, K. Svennersten-Sjaunja, J.-E. Haugen, F. Lundby, O. Lind, *Int. Dairy J.* **2005**, *15*, 1193.
- [297] J. K. Carrillo-Gómez, C. M. D. Acevedo, R. O. García-Rico, *Sens. Biosens. Res.* **2021**, *33*, 100428.
- [298] J. A. Ragazzo-Sanchez, P. Chaliar, D. Chevalier-Lucia, M. Calderon-Santoyo, C. Ghommidh, *Sens. Actuators, B* **2009**, *140*, 29.
- [299] S. Buratti, D. Ballabio, S. Benedetti, M. S. Cosio, *Food Chem.* **2007**, *100*, 211.
- [300] J. Lozano, T. Arroyo, J. P. Santos, J. M. Cabellos, M. C. Horrillo, *Sens. Actuators, B* **2008**, *133*, 180.
- [301] H. Yu, Y. Wang, J. Wang, *Sensors* **2009**, *9*, 8073.
- [302] N. Bhattacharya, B. Tudu, A. Jana, D. Ghosh, R. Bandhopadhyaya, M. Bhuyan, *Sens. Actuators, B* **2008**, *131*, 110.
- [303] B. Tudu, A. Jana, A. Metla, D. Ghosh, N. Bhattacharyya, R. Bandyopadhyay, *Sens. Actuators, B* **2009**, *138*, 90.
- [304] J. Rodríguez, C. Durán, A. Reyes, *Sensors* **2010**, *10*, 36.
- [305] M. Wang, F. Gao, Q. Wu, J. Zhang, Y. Xue, H. Wan, P. Wang, *Anal. Methods* **2018**, *10*, 4741.
- [306] V. Schroeder, E. D. Evans, Y.-C. M. Wu, C.-C. A. Voll, B. R. McDonald, S. Savagatrup, T. M. Swager, *ACS Sens.* **2019**, *4*, 2101.
- [307] Z. Yuan, M. Bariya, H. M. Fahad, J. Wu, R. Han, N. Gupta, A. Javey, *Adv. Mater.* **2020**, *32*, 1908385.
- [308] H. Yousefi, H.-M. Su, S. M. Imani, K. Alkhalidi, C. D. M. Filipe, T. F. Didar, *ACS Sens.* **2019**, *4*, 808.
- [309] M. Weston, S. Geng, R. Chandrawati, *Adv. Mater. Technol.* **2021**, *6*, 2001242.
- [310] F. Mustafa, S. Andreescu, *RSC Adv.* **2020**, *10*, 19309.
- [311] M. K. Morsy, K. Zór, N. Kostashe, T. S. Alstrøm, A. Heiskanen, H. El-Tanahi, A. Sharoba, D. Papkovsky, J. Larsen, H. Khalaf, M. H. Jakobsen, J. Emnéus, *Food Control* **2016**, *60*, 346.
- [312] F. Saliu, R. D. Pergola, *Sens. Actuators, B* **2018**, *258*, 1117.
- [313] R. Wu, L. Tian, H. Li, H. Liu, J. Luo, X. Tian, Z. Hua, Y. Wu, S. Fan, *Sens. Actuators, B* **2022**, *359*, 131557.
- [314] Y. Chen, G. Fu, Y. Zilberman, W. Ruan, S. K. Ameri, Y. S. Zhang, E. Miller, S. R. Sonkusale, *Food Control* **2017**, *82*, 227.
- [315] M. Serasanambati, Y. Y. Broza, A. Marmur, H. Haick, *iScience* **2019**, *11*, 178.
- [316] J. Dummer, M. Storer, M. Swanney, M. McEwan, A. Scott-Thomas, S. Bhandari, S. Chambers, R. Dweik, M. Epton, *TrAC-Trends Anal. Chem.* **2011**, *30*, 960.
- [317] R. S. Beach, J. A. Borchers, A. Matheny, R. W. Erwin, M. B. Salaman, B. Everitt, K. Pettit, J. J. Rhyne, C. P. Flynn, *Phys. Rev. Lett.* **1993**, *70*, 3502.
- [318] R. E. Amor, M. K. Nakhleh, O. Barash, H. Haick, *Eur. Respir. Rev.* **2019**, *28*, 190002.
- [319] C. Di Natale, A. Macagnano, E. Martinelli, R. Paolesse, G. D'Arcangelo, C. Roscioni, A. Finazzi-Agrò, A. D'Amico, *Biosens. Bioelectron.* **2003**, *18*, 1209.
- [320] M. Murdocca, F. Torino, S. Pucci, M. Costantini, R. Capuano, C. Greggi, C. Polidoro, G. Somma, V. Pasqualetti, Y. K. Mougang, A. Catini, G. Simone, R. Paolesse, A. Orlandi, A. Mauriello, M. Roselli, A. Magrini, G. Novelli, C. Di Natale, F. C. Sangiuolo, *Cancers* **2021**, *13*, 4213.
- [321] Y. K. Mougang, L. Di Zazzo, M. Minieri, R. Capuano, A. Catini, J. M. Legramante, R. Paolesse, S. Bernardini, C. Di Natale, *iScience* **2021**, *24*, 102851.
- [322] G. Konvalina, H. Haick, *Acc. Chem. Res.* **2014**, *47*, 66.
- [323] H. Amal, M. Leja, K. Funke, I. Lasina, R. Skapars, A. Sivins, G. Ancans, I. Kikuste, A. Vanags, I. Tolmanis, A. Kirsners, L. Kupcinkas, H. Haick, *Int. J. Cancer* **2016**, *138*, 229.
- [324] Z.-Q. Xu, Y. Y. Broza, R. Ionsecu, U. Tisch, L. Ding, H. Liu, Q. Song, Y.-Y. Pan, F.-X. Xiong, K.-S. Gu, G.-P. Sun, Z.-D. Chen, M. Leja, H. Haick, *Br. J. Cancer* **2013**, *108*, 941.
- [325] L. Wei, J. Sun, L. Xu, S. D. Zhu, X. Y. Zhou, S. Yang, B. Dong, X. Bai, G. Lu, H. Song, *Nanoscale Horiz.* **2019**, *4*, 1361.
- [326] G. Peng, U. Tisch, O. Adams, M. Hakim, N. Shehada, Y. Y. Broza, S. Billan, R. Abdah-Bortnyak, A. Kuten, H. Haick, *Nat. Nanotechnol.* **2009**, *4*, 669.
- [327] T. Saidi, O. Zaim, M. Moufid, N. El Bari, R. Ionescu, B. Bouchikhi, *Sens. Actuators, B* **2018**, *257*, 178.
- [328] M. Righettoni, A. Amann, S. E. Pratsinis, *Mater. Today* **2015**, *18*, 163.
- [329] Y. Adiguzel, H. Kulah, *Biosens. Bioelectron.* **2015**, *65*, 121.
- [330] G. Peng, M. Hakim, Y. Y. Broza, S. Billan, R. Abdah-Bortnyak, A. Kuten, U. Tisch, H. Haick, *Br. J. Cancer* **2010**, *103*, 542.
- [331] X. Chen, F. Xu, Y. Wang, Y. Pan, D. Lu, P. Wang, K. Ying, E. Chen, W. Zhang, *Cancer* **2007**, *110*, 835.
- [332] R. Thriumani, A. Zakaria, Y. Z. H.-Y. Hashim, A. I. Jeffree, K. M. Helmy, L. M. Kamarudin, M. I. Omar, A. Y. M. Shakaff, A. H. Adom, K. C. Persaud, *BMC Cancer* **2018**, *18*, 362.
- [333] K. Schallschmidt, R. Becker, C. Jung, W. Bremser, T. Walles, J. Neudecker, G. Leschber, S. Frese, I. Nehls, *J. Breath Res.* **2016**, *10*, 046007.
- [334] T. Oguma, T. Nagaoka, M. Kurahashi, N. Kobayashi, S. Yamamori, C. Tsuji, H. Takiguchi, K. Niimi, H. Tomomatsu, K. Tomomatsu, N. Hayama, T. Aoki, T. Urano, K. Magatani, S. Takeda, T. Abe, K. Asano, *PLoS One* **2017**, *12*, e0174802.
- [335] R. Capuano, M. Santonico, G. Pennazza, S. Ghezzi, E. Martinelli, C. Roscioni, G. Lucantoni, G. Galluccio, R. Paolesse, C. Di Natale, A. D'Amico, *Sci. Rep.* **2015**, *5*, 16491.

- [336] L. Liu, T. Fei, X. Guan, H. Zhao, T. Zhang, *Biosens. Bioelectron.* **2021**, *191*, 113459.
- [337] K. Toma, M. Tsujii, T. Arakawa, Y. Iwasaki, K. Mitsubayashi, *Sens. Actuators, B* **2021**, *329*, 129260.
- [338] G. Konvalina, H. Haick, *Acc. Chem. Res.* **2014**, *47*, 66.
- [339] S. P. Schon, S. J. Theodore, A. T. Güntner, *Sens. Actuators, B* **2018**, *273*, 1780.
- [340] Z. Wu, X. Yang, J. Wu, *ACS Appl. Mater. Interfaces* **2021**, *13*, 2128.
- [341] M. K. Nakhleh, H. Amal, R. Jeries, Y. Y. Broza, M. Aboud, A. Gharra, H. Ivgi, S. Khatib, S. Badarneh, L. Har-Shai, L. Glass-Marmor, I. Lejbkovicz, A. Miller, S. Badarny, R. Winer, J. Finberg, S. Cohen-Kaminsky, F. Perros, D. Montani, B. Girerd, G. Garcia, G. Simonneau, F. Nakhoul, S. Baram, R. Salim, M. Hakim, M. Gruber, O. Ronen, T. Marshak, I. Doweck, et al, *ACS Nano* **2017**, *11*, 112.



Angelo Milone (1994) graduated in Physics (magna cum laude) in 2018 at University of Salento and got degree from the school of excellence ISUFI in 2019 (magna cum laude). In 2018 he interned at IBM Almaden – Research for a joint project between University of Salento and IBM, working on the “*Optimization of Sensors for Volatile Organic Compounds detection*”. From 2018 to 2021, he was PhD student at University of Salento and CNR Nanotec within the Omnics research group. In 2022, he obtained his Ph.D. (excellent cum laude), defending a thesis entitled “*Engineered and reconfigurable gas sensors for monitoring and diagnostic applications.*”



Anna Grazia Monteduro is researcher at the Department of Mathematics and Physics of University of Salento and carries out her research activity within Omnics Research Group in the fields of (i) sensors and lab on chip; (ii) Nanoelectronics, spintronics and nanomagnetism. From 2016 to 2018, she worked in collaboration with the National Institute of Research in Gastroenterology “Saverio De Bellis” – IRCCS, Castellana Grotte (BA) for the development of biosensoristic and Lab-on-chip devices within a project on “*Personalized therapy in patients with liver tumor*”.



Silvia Rizzato is researcher at the Department of Mathematics and Physics of University of Salento and carries out her research activity within Omnics Research Group. Her research activity is focused on the development of new devices and processes for sensing and spintronics. In particular, she works on surface acoustic waves devices, electrochemical sensors and colloidal lithography for LSPR sensors. She has also expertise in lithography, preparation and processing of magnetoresistive sensors and their characterization by means of magnetotransport experiments.



Angelo Leo is researcher at the Department of Mathematics and Physics of University of Salento. He got PhD in Physics and Nanoscience on December 2014. After a post-doc stage in ST Microelectronics, in which he worked on the development of platforms for biomedical and microelectronics applications, he is actually engaged in the optimization of devices for liquid biopsy and in the fields of magnonics and spintronics.



Corrado Di Natale is Full professor of Electronics at the Department of Electronic Engineering of the University of Rome Tor Vergata. His research activities are concerned with the development and application of chemical sensors, bio-sensors, and artificial sensorial systems (olfaction and taste), and with the study of the optical and electronic properties of organic and molecular materials. Corrado Di Natale authored more than 300 papers on international journals and conference proceedings (14173 citations, H-index=64, source Scopus). He has been member of the organizing committees of National and International conferences in sensors. He serves in the steering committee of the Eurosensors conferences series and he is the current of the chairman of the Italian Association on Sensors and Microsystems.



Sang Sub Kim joined the Department of Materials Science and Engineering, Inha University, in 2007 as a full professor. He received his B.S. degree from Seoul National University and his M.S and Ph.D. degrees from Pohang University of Science and Technology (POSTECH) in Material Science and Engineering in 1987, 1990, and 1994, respectively. He was a visiting researcher at the National Research in Inorganic Materials (currently NIMS), Japan for 2 years each in 1995 and in 2000. In 2006, he was a visiting professor at Department of Chemistry, University of Alberta, Canada. In 2010, he also served as a cooperative professor at Nagaoka University of Technology, Japan. His research interests include the synthesis and applications of nanomaterials such as nanowires and nanofibers, functional thin films, and surface and interfacial characterizations.



Giuseppe Maruccio (1978) is Full Professor in Physics of Matter (FIS/03) at the Dept. of Mathematics and Physics – University of Salento and head of the Omnic Research Group which comprises researchers with different backgrounds from physics to life sciences working in close collaboration to foster exploratory and seeding research in cross-disciplinary areas with applications spanning from -onics (electronics, spintronics and magnonics) to -omics technologies (genomics, proteomics and cellomics). Omnic laboratories represent the Italian node of the European Infrastructure on Magnetism funded within the ISABEL project (H2020-INFRADEV-2018-2020) and are part of the Italian Innovative Research Infrastructure on applied Superconductivity (IRIS).